SEISMIC DATA LABORATORY

SEMI-ANNUAL TECHNICAL SUMMARY REPORT

15 April 1965

Prepared For

Code 1

AIR FORCE TECHNICAL APPLICATIONS CENTER
Washington, D. C.

By

UED EARTH SCIENCES DIVISION
TELEDYNE, INC.

Under

Project VELA UNIFORM

Sponsored By

ADVANCED RESEARCH PROJECTS AGENCY
Nuclear Test Detection Office
ARPA Order No. 624

SEISMIC DATA LABORATORY
SEMI-ANNUAL TECHNICAL
SUMMARY REPORT

15 April 1965

AFTAC Project No.:	VELA T/2037
Project Title:	Seismic Data Laboratory
Authority No.:	624
ARPA Program Code No.:	5810
Name of Contractor:	UED EARTH SCIENCES DIVISION TELEDYNE, INC.
Contract No.:	AF 33(657) 12447
Date of Contract:	17 August 1963
Amount of Contract:	$5,257,624
Contract Expiration Date:	17 February 1966
Project Manager:	Robert Van Nostrand (703) 836-7644

P. O. Box 334, Alexandria, Virginia

This research was supported by the Advanced Research Projects Agency, Nuclear Test Detection Office, and was monitored by the Air Force Technical Applications Center under Contract AF 33(657) 12447.

TABLE OF CONTENTS

TABLE OF CONTENTS (Continued)

LIST OF ILLUSTRATIONS

LIST OF ILLUSTRATIONS (Continued)

I. INTRODUCTION

This is the seventh semi-annual report and covers work performed from October 1964 through March 1965. During this period, an amendment was negotiated to extend contract AF33(657)-12447 from 17 February 1965 through 17 February 1966. Under terms of this amendment, semi-annual reports will be replaced by quarterly reports; the present report combines the semi-annual previously required and the first quarterly report required under the amended contract.

Specific analyses made, for which results have been reported to AFTAC, are discussed in Section II under descriptive headings; work currently in progress, which has not reached the stage where results are available, is discussed in Section IV, Work previously completed is mentioned only as it relates to analyses in progress during this reporting period.

II. WORK COMPLETED

A. Analysis of Signal Variance

The purpose of the present work has been to give a technical evaluation of the analysis of variance as a method of automatic signal detection. The analysis of variance has been programmed for the digital computer and the resulting program may be considered an array processor for the purpose of signal detection only.

The analysis of variance considered as a method of signal detection by Melton and Bailey[1] depends upon the similarity of signals across channels, as compared to the noise, for array recorded data. For weak signals, prefiltering is necessary as the similarity of the long-period noise across the array dominates the results. Thus, the computational task is to filter out the long-period noise, hopefully leaving only incoherent noise across channels. Then the analysis of variance computation provides an output function of time which measures the likelihood of a signal being present in the noise.

One important feature of the above detection technique is a lack of assumptions about the signal. Most of the classical

[1] Melton, Ben S. and Bailey, Leslie F., "Multiple Signal Correlators," Geophysics, Vol. XXII, No. 3, July 1957.

work[2] in optimum filtering or detection theory assumes that both signal and noise are stochastic processes with known spectra. The resulting optimum processing was given by Weiner. If one assumes the signal is a fixed known wavelet, then the optimum filter is called a matched filter. Modifications of the above techniques have been studies, such as assuming that the signal is repeating in the noise or is known apart from a set of parameters which have to be estimated from the data. None of these techniques provides a suitable basic assumption regarding seismic signals. If the signal trace is regarded as a stochastic process then it is non-stationary and zero with high probability. If the signal trace is considered deterministic, then the variation due to recording station, epicenter location, or type of event is difficult to model with a relatively small number of parameters. Consequently, it is considered desirable to examine those techniques which make no assumptions at all regarding the signal.

The logical steps of computation for the method of detection considered in this study were subsetting data, signal addition, filtering, and analysis of variance computation. These steps have been programmed individually and combined into a single program by a system called "FLAP".

The basic operation the program must repeatedly make is to compute Fisher's F statistic for testing the hypothesis that no column effects (no signal) exist in a 2-way table with one observation per cell is given by:

$$F = \frac{s(r-1)}{r(s-1)} \quad \frac{\sum_{j=1}^{s}\left(\sum_{i=1}^{r} y_{ij}\right)^2 - s^{-1}\left(\sum_{ij} y_{ij}\right)^2}{\sum_{ij} y_{ij}^2 - r^{-1}\sum_{j}\left(\sum_{i} y_{ij}\right)^2}$$

where y_{ij} is the observed value for the i^{th} channel, and the j^{th} sampling time, r the number of channels, and s the number of time increments at which samples are measured.

[2] Helstrom, C. W., Statistical Theory of Signal Detection, Pergamon Press, 1960.

Several parameters such as sampling rate, bard pass filtering, and signal-to-noise ratio were tested for effect on the computation of F. From the following table, the effect of changing the sampling rate is seen to be minimal.

DATA SAMPLE (Filtered TFO Noise)

SAMPLING RATE (Samples Per Second)	1	2	3	4
100	1.94	2.16	2.24	1.35
50	1.94	2.17	2.24	1.35
20	1.95	2.19	2.25	1.35
10	1.98	2.21	2.27	1.35

DATA SAMPLE (Filtered TFO Signal and Noise)

	1	2	3	4
100	47.31	67.58	36.60	43.1[illegible]
50	47.40	67.70	36.70	43.30
20	47.65	68.13	36.87	43.49
10	48.51	68.88	37.23	43.78

Effect of Sampling Rate on F

It is clear that 100 samples per second is unnecessary. In fact, the results indicate that 10 samples per second is sufficiently accurate and the effective sampling rate was frozen at this value for the remainder of the results.

From results of applying the detection procedure to raw data and band-pass filtered data, it was obvious that filtering is a critical part of the method. The band-pass

filter with cut-offs at 0.75 cps and 4 cps was selected as standard for the present report. Similarly, several values of window width were tried with the expected result that the optimum window width is the length of the signal.

Figure 1 illustrates the effect of S/N ratios on F computations with signals of varying complexity at several stations.

The F's were calculated using 5 second windows which included the array stations first second of signal plus 4 seconds of preceding noise. In general the slope of the curves for simpler signals is greater, but, in any case, the expected contrast in F values can be expected to be appreciably greater than the S/N ratio itself. The background noise given on the figure is an average of 23 values of F for the noise preceding the signal.

Eighteen teleseismic signals were selected on the basis of small signal-to-noise ratios. No velocity filtering was done before processing. Three examples of the results are shown in Figure 2. In each case, the dotted trace gives the F values and the solid trace the unphased sum of all seismograms from the array. Timing lines are spaced at 5-second intervals.

In an automatic detection system, one would have to assume some critical value F_c above which the F-trace would sound an alarm. In this experiment, the theoretical false alarm rate was surpassed somewhat. This was to be expected as we knew the band-pass filtering would not completely eliminate the correlations in time, and yet our assumptions were that the observations in time are uncorrelated. One should be able to adjust the critical values to take into consideration this correlation. This problem has been considered in the literature by G. E. P. Box[3] for correlations extended only one unit and some calculations were necessary to extend this theory to the present problem.

We also studied the effects of velocity filtering the data before computing F values.

[3] Box, G. E. P., "Some Theorems on Quadratic Forms Applied in the Study of Analysis of Variance Problems, II. Effects of Inequality of Variance and of Correlation Between Errors in the Two-Way Calssification," Annals of Mathematical Statistics, 25:484-498, 1954.

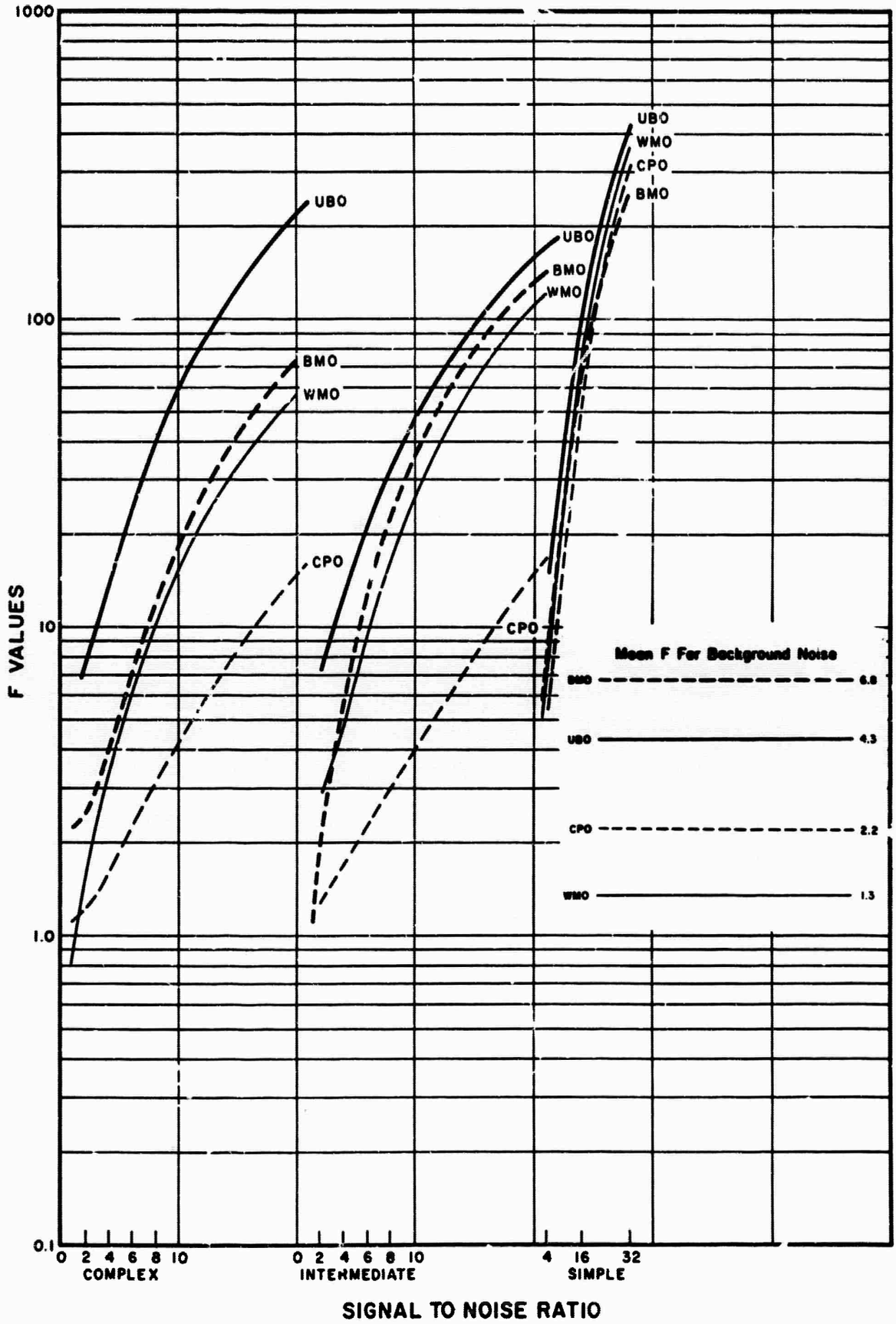

Increase In F As A Function Of S/N

Figure 1

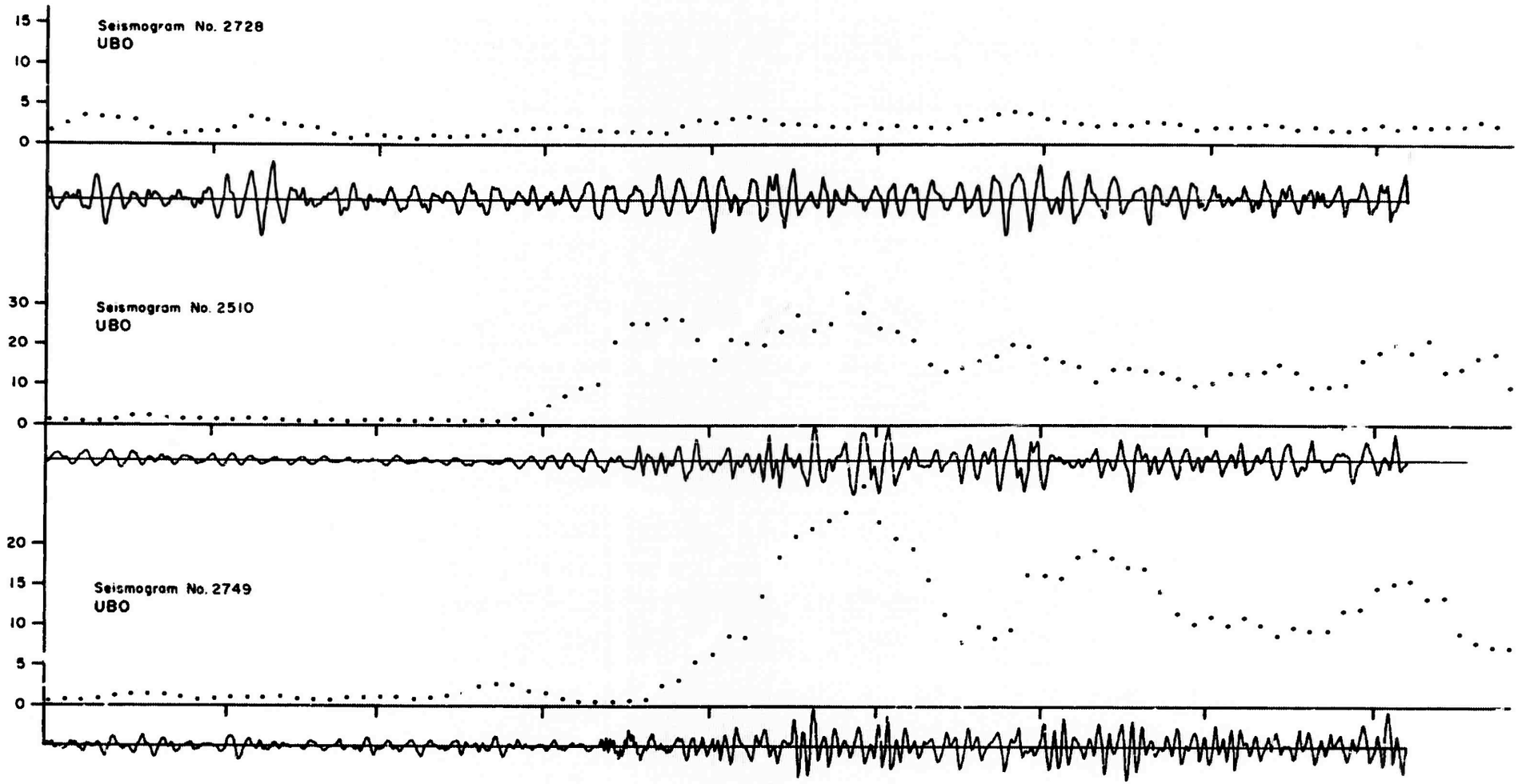

F Values and Corresponding Array Sums for Teleseismic Signals

Figure 2

The results indicated that time-shifting the data is not essential for the detection procedure, although significant improvement may be possible for some signals at low apparent velocities. The cost of this improvement is that F values for a grid of velocities and epicentral azimuth would have to be computed for each window of data. More work is needed to ascertain whether the gain will justify this cost, although in some cases when an operational array is to be beamed at a single epicentral region, the additional cost would be minimized.

We have concluded that the method of signal detection examined is very effective when the background noise is incoherent in the frequency band of interest. The background noise seemed to satisfy this criterion with the exception of TFO where the average background values of F were at least two times the average values at the other arrays. This may be due to a completely different character of the noise field at TFO.

There is evidence that very accurate shifting would improve the significance of the F values. Not only are the F values increased due to shifting when signals are present, but the background noise values are systematically reduced by shifting in the absence of signal. The present program computes the shift in units of 0.05 seconds and truncates to the nearest integer. Future programs should be written to interpolate as an option to allow a more accurate view of the effect of time shifting.

The large increase in S/N for the F "seismogram" has been seen by comparing the peak values of F to the mean background values. The parameter χ^2 was also studied for comparison. Although the detectors F and χ^2 were both effective as detectors for the data examined, the F peak values exceeded the mean background values by a consistantly larger number of standard deviations than did the χ^2. The F criteria is amplitude-dependent where the χ^2 values are not. Thus, one would expect the F detector to be better for strong signals. The data show the F values are better for weak signals as well. Unless there are other compelling reasons, such as cost of computation or possiblity of on-line computation of χ^2 and not

F, the results of this report confirm the theoretical result that F should be an optimum detection criterion.

The following work is recommended if the F method is to be considered further for noise elimination with the LASA data:

1. Re-program the analysis of variance making the following changes:

   A. The filtering should be made an integral part of the analysis of variance computation.

   B. The program should handle a maximum of 525 channels with the computation being done "in time", i.e., the calculations necessary for a vector of observations at a given point in time should be completed at once, then the next vector in time processed, and so on.

   C. Shifting with interpolation should be included as an option.

   D. The program should be written for use on the 1604 but with the idea in mind that the same flow charts and analysis would be suitable, with minor changes, for programming the on-line system at LASA.

2. The program described in (1) should be used to investigate sensitivity to velocity phasing on larger arrays.

3. The existing program should be used to study various filters for the different arrays. Optimum single channel filtering in frequency could be used and the results compared with those of the present report. (Optimum multi-channel filtering may introduce correlations across channels.)

B. Solutions of the General Wave Equation

Midway in the current reporting peri[illegible] formal work on

this project was suspended indefinitely in favor of studies that bear promise of more immediate benefit to the detection-identification problem. However, several significant results were reported before the work was terminated.

Green's function for the reduced wave equation (Helmholtz equation) in a spherical annular domain with Dirichlet boundary conditions was derived. The convergence of the series solution, representing Green's function, was then established. Finally, it was shown that Green's function of the Dirichlet problem reduces to Green's function for the exterior of a sphere as given by Franz and Etiènne[4], when the outer radius is moved towards infinity, and when a special position of the cooredinate system is chosen.

Green's function has been constructed here in reference to an asymmetrically located coordinate system, different from Franz's and Etienne's results where an axial symmetric position was employed. The reason for this generalization lies in the fact that in contrast to axial symmetric systems, disturbance fields due to earthquakes, for example, are most probably not axially symmetric relative to the approximate spherical shape of the earth. This type of Green's function permits construction of any general asymmetric discrete source system inside a spherical layer Therefore, a comparison of at least pure steady state body waves and their scattering characteristics inside fluid sphere layers with free boundaries, where the waves are created from point symmetric or axially symmetric sources on the one hand, and asymmetric sources on the other hand, can now be made. According to an idea advanced by Jeffreys, this comparison indicates the body wave scattering characteristics occuring in elastic spheres.

The corresponding solutions and proofs were given for a circular annular domain with the Dirichlet, the radiation (mixed), and Neumann boundary conditions being derived. The convergence of the series representing Green's functions was then established. Finally it was shown that these functions reduce to Green's function for the exterior of a circle as given by Franz and Etiènne, when the outer radius is moved towards infinity.

---

[4]Etiènne, J., "Fonction de Green de l'operateur métaharmonique pour les problèmes de Dirichlet ou de Neumann a'linterieur d'um cercle ou d'um sphere "Bull Soc. Roy. des Sciences de Liège. Vol. 30, 1961, pp. 416-426.

Currently, in seismology, numerical analysis is applied to obtain normal mode solutions for propagating waves in a plane, parallel homogeneously layered structure. The solutions are obtained rapidly and with high accuracy. More recently, normal mode solutions in a spherical earth model have been obtained numerically for spheres composed of concentric shells. However, in this case, there was considerable difficulty in obtaining solutions rapidly and accurately. The main difficulties were posed by the requirement of an excessive number of shells to accurately represent the whole interior of the earth, and computational difficulties in evaluating Bessel functions with sufficient accuracy, especially at high frequencies. We conducted an analyis to explore two avenues toward alleviating these difficulties. In particular we:

1. Represented the elastic parameters in each shell as continuously variable quantities in order to greatly reduce the number of shells required to accurately represent the interior of the earth.

2. Rigorously evaluated a transformation through which a solution in plane parallel layers could be utilized to approximate the solution for spherical shells.

In the latter case, a special kind of inhomogeneous medium has been analyzed in which the reciprocal radii transformation for spherical inversion is invariant with respect to the reduced wave equation describing the motion in a sphere. Thus, by transforming a shell from a region inside of a large inversion sphere to a region outside that sphere, the boundary conditions can be accurately represented by those for plane parallel layers. In particular, if pseudo amplitudes are defined as

$$C'_1 = C_1 \exp\left(\frac{-z'}{2a}\right)$$

$$C'_2 = C_2 \exp\left(\frac{-z'}{2a}\right)$$

and a pseudo velocity is defined as

$$\frac{1}{\gamma'^2} = \rho_0 \eta^2 - \frac{1}{4a^2\omega^2} \quad ,$$

where a is the radius of the inversion sphere, γ either the shear or compressional propagation velocity, ρ the density, and ω the angular frequency, the wave potential is reduced exactly to the form of a plane wave potential in a flat layered structure, as follows:

$$R(z') = C'_1 \exp\left(ik\sqrt{\frac{c^2}{\gamma'^2} - 1}\; z'\right)$$

$$+ C'_2 \exp\left(-ik\sqrt{\frac{c^2}{\gamma'^2} - 1}\; z'\right), \quad (0 \leq z' < \infty)$$

Haskell's[5] exact method for plane parallel layers can now be applied in principle to obtain the approximate solution of a layered elastic sphere. To obtain free periods of oscillation of the layered sphere we take $a^2k^2 = n(n+1)$, which for each wave mode specified by $C_i(\omega)$ leads to eigenfrequencies given by roots of the equation $n(n+1)\frac{C_i(\omega)^2}{a^2} - \omega^2 = 0$. The completeness of the exact solutions obtained using Haskell's method will depend upon the treatment of the boundary condition at infinity, which corresponds to $r = 0$ in the region $0 \leq r \leq a$.

It is important to remember that Sommerfeld showed that spherical inversion cannot be applied to the usual Helmholtz equation. Here it has been shown that spherical inversion can be applied to at least one special case of the reduced wave equation with variable elastic parameters.

In order to determine the effect of diffraction around the earth's core, we studied SH waves in a model consisting of a single spherical elastic layer which surrounds a liquid core. We considered two SH sources located inside the elastic layer, such that the field, due to the sources, is axial symmetric and steady state. Thus, the sources have been assumed in a form which assures equilibrium of the elastic fluid system at all times. The effect of gravity has been neglected.

[5] Haskell, N. Q., The dispersion of surface waves in multilayered media, in Bull. Seismol. Soc. Amer., 43, 17-34, 1953.

We commenced by deriving the exact solution due to a single SH source in form of Green's function and investigating the denominator D of this series solution in relation to the complex Watson integral. The consideration of a single SH source was here sufficient as all other SH source distributions were immediately obtained by superposition. For this purpose, it was necessary to consider the Green's function as a function of the index, which now appears as an independent variable, and to study those indices of the functions appearing in D for which D vanishes. Calling the index of the functions appearing in D "ν", it was demonstrated that the ν-zeros of D were similar to the ones obtained for the Green's function for the reduced wave equation in an annular domain and in a spherical layer with Dirichlet's, Neumann's, or mixed boundary conditions. The ν-zeros were found to be either real or complex. Futhermore, for real arguments of the functions appearing in D, it was established that D had a countable number of ν-zeros of which only at most a finite number were real. All of these ν-zeros were shown to be simple, except for that which occurred at $a_2 = -\frac{1}{2}$, which can appear only as a zero of the second order. Asymptotic expressions were then derived for the two dimensional counterpart for large imaginary ν-zeros.

In addition, it was proven that there are no real ν-zeros for arbitrarily large modulus. Also, D was found to be neither an odd nor even function of ν for the general case; however, symmetry of the ν-zeros with respect to the real ν-axis, of course, does exist. The conclusion drawn from these studies on the ν-zeros indicates that the Watson transformation is only directly applicable in those physical situations where there are no real ν-zeros. For these special cases a core comparison is then carried out, whereby the two-dimensional counterpart to the real three-dimensional elasticity problem has been chosen for reasons of simplicity. These studies reveal that the only difference for certain simple core changes, namely $\tau_{ry} = 0$ compared to $\tau_{ry} \neq 0$, is essentially a shift in the pure imaginary ν-zeros along that axis. In this instance, the distribution of the imaginary ν-zeros is hardly effected.

In comparison, in problems in seismology, for the type of layer and core, and nature of source considered here, the waves are unattenuated. Also, due to the periods, wave numbers, etc.. of

the waves which occur in the earth, and the dimensions of the layers, only real ν-zeros exist here. In this situation, like in the one considered above, where there are only complex (in three dimensions) or purely imaginary (in two dimensions) ν-zeros, the elastic layer acts as a waveguide. This is due to the fact that there are no shear waves transmitted to the outside of the layer nor into the core. In these cases, the Watson transformation is no longer directly applicable to the complete solution. A decomposition of the complete solution is therefore carried out on similar lines as was done by Van der Pol and Bremmer[6] by constructing the solution anew in terms of infinite sums of reflections inside the layer with the aid of reflection coefficients. These coefficients are consequently computed and it is shown that Watson's transformation can now be again applied to each term of the new series, as the individual terms of the new series are finally free of real ν-zeros. In order to facilitate the application of the Watson transformation to expressions with multiple ν-zeros, which characterize the terms of the new series, the necessary formula based on Cauchy's theorem and the Laurent expansion is derived.

In conclusion, a concise analysis of the Cauchy formula and the Laurent expansion yielding the residues has been given, as the residues in a layer problem are much more complicated than the residues in problems with a single surface boundary. The method derived in this work brings the problem to a stage where numerical computations can now be contemplated. This is possible because each of the denominators of the geometric series terms has now ν-zeros whose analysis has been performed earlier in other investigations (Duvalo - Jacobs)[7]. With this result it is finally possible to separate approximately surface (diffraction) waves from reflected waves and determine their nature and characteristic features.

C. Model Studies

We have an operational program to model the effect of reverberation of teleseismic signals in the crust, both at receiver

[6] Van der Pol, and Bremmer, H., 1937, Phil. Mag., Ser. 7, Vol. 24, p. 141, and p. 825.

[7] Duvalo, G., and Jacobs, J. A., 1959, Can. Journ. Phys., Vol. 37, p. 109.

and the source. Although we are no longer doing development work, we have used this program to demonstrate some simple, albeit general, conclusions concerning teleseismic signals.

The wave forms in Figure 3 were plotted to furnish an elementary insight into the effect of the free surface on the primary wave from a shallow explosion.

The wave forms shown in the upper half of Figure 3 are simply the sum of two identical wavelets, one of which is inverted and delayed by the intervals shown (Δt). The results are interpreted to be simulated downward travelling P-pulses, perturbed by the surface reflected pP-pulses. Inasmuch as the apparent period of the basic wavelet is one second, the delay times may be interpreted as the two-way travel paths from the explosion to the earth's surface, expressed as fractions of wavelengths.

An analogous set of signals is shown in the lower half of Figure 3, in which the two signals are added in phase and delayed as before. These wave forms may be interpreted as incoming teleseisms, originally of the same simple pulse shape, recorded at depth below the free surface.

Although the wave shape varies considerably as a function of depth, there is no quantity or characteristic which can be measured and related to depth. The only way to relate wave shape to depth for the comparatively shallow events depicted in this exercise would be to match wave forms. This technique also would probably be unsuccessful in practice due to complications beyond our control.

In a similar exercise, we have studied the possible effects of reverberation on signal amplitude. When the signal amplitude recorded at each of several stations for a given event is plotted as a function of the epicentral distance, there is considerable scatter in the data. The same is true even when special care is taken to insure that the points represent the arrivals of the same single phase. It was the purpose of this study to investigate in a very simple way what possible variation in signal amplitude we might reasonably expect from changes in the near surface rocks and, in particular, from changes in the

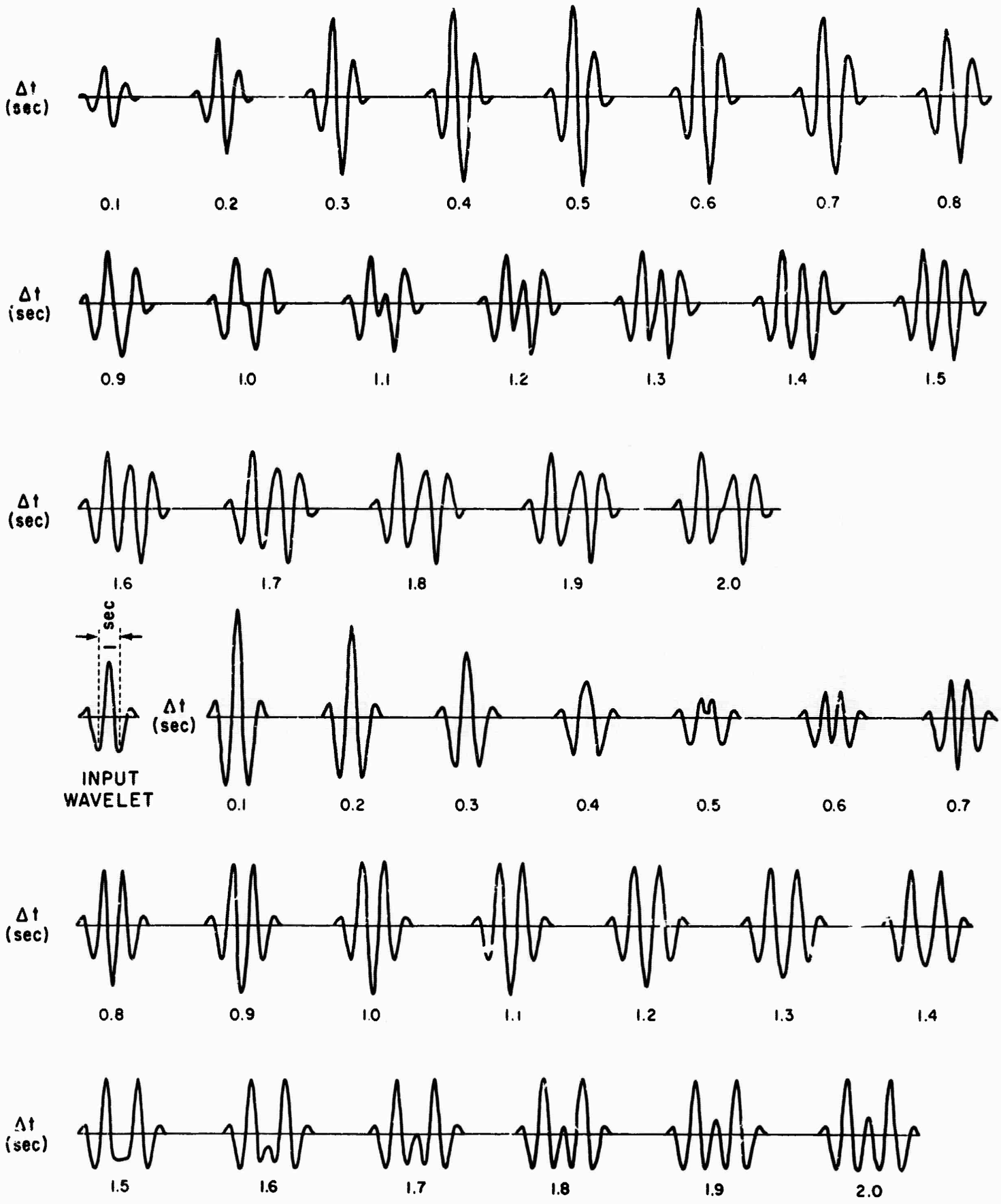

Effect of Free Surface On Teleseismic Signals Assumed to Originate as a Ricker Wavelet

Figure 3

sedimentary section from station to station

The basic contributing unit in the geologic section is obviously the single stratigraphic layer and we are intuitively led to believe that the most important layer is the surface layer where the topside reflection coefficient is unity or, in practice at least, near unity. Therefore, we commenced our study with a single uniform layer. The density within the layer is 2.35 grams per cubic centimeter and the velocity of compressional waves is 3.1 km per second. In the underlying material the corresponding density and velocity are 2.60 and 6.03.

Figure 4 shows the effect on the amplitude of the signal at the surface; the amplitudes are normalized so that the amplitude for zero thichness is unity and the thicknesses are measured in terms of wavelength λ. We could have predicted that we would have obtained a maximum for a resonant thickness equal to quarter-wavelength and this curve indicates how large the maximum amplitude is. For velocities shown in Model 1, and for teleseisms peaking at one cycle per second, the quarter-wavelength resonant thickness is 775 meters and the signal amplitude is up 91% over its level, were the top layer completely removed. It should be noted that the amplitude in question is the maximum peak-to-peak amplitude which is usually measured from the first peak to the second trough.

Having verified that the maximum amplitude occurs at a quarter-wavelength thickness, it is now useful to examine how the amplitude varies when the acoustic impedance is changed. To gain insight into this problem, we repeated the first exercise, simply changing the density and compressional velocity in the upper layer to 2.15 and 2.0. These are about the lower limits of the parameters that are found for a reasonably thick surface layer in nature. The results are also shown in Figure 4. As in the first case, the maximum amplitude occurs at a thickness equal to the quarter-wavelength. However, the amplitude at the maximum has changed, as has the amplitude for thicknesses of the order of a wavelength and larger.

The limiting amplitude for large thicknesses is obviously governed by the acoustic impedance; the ratio of the

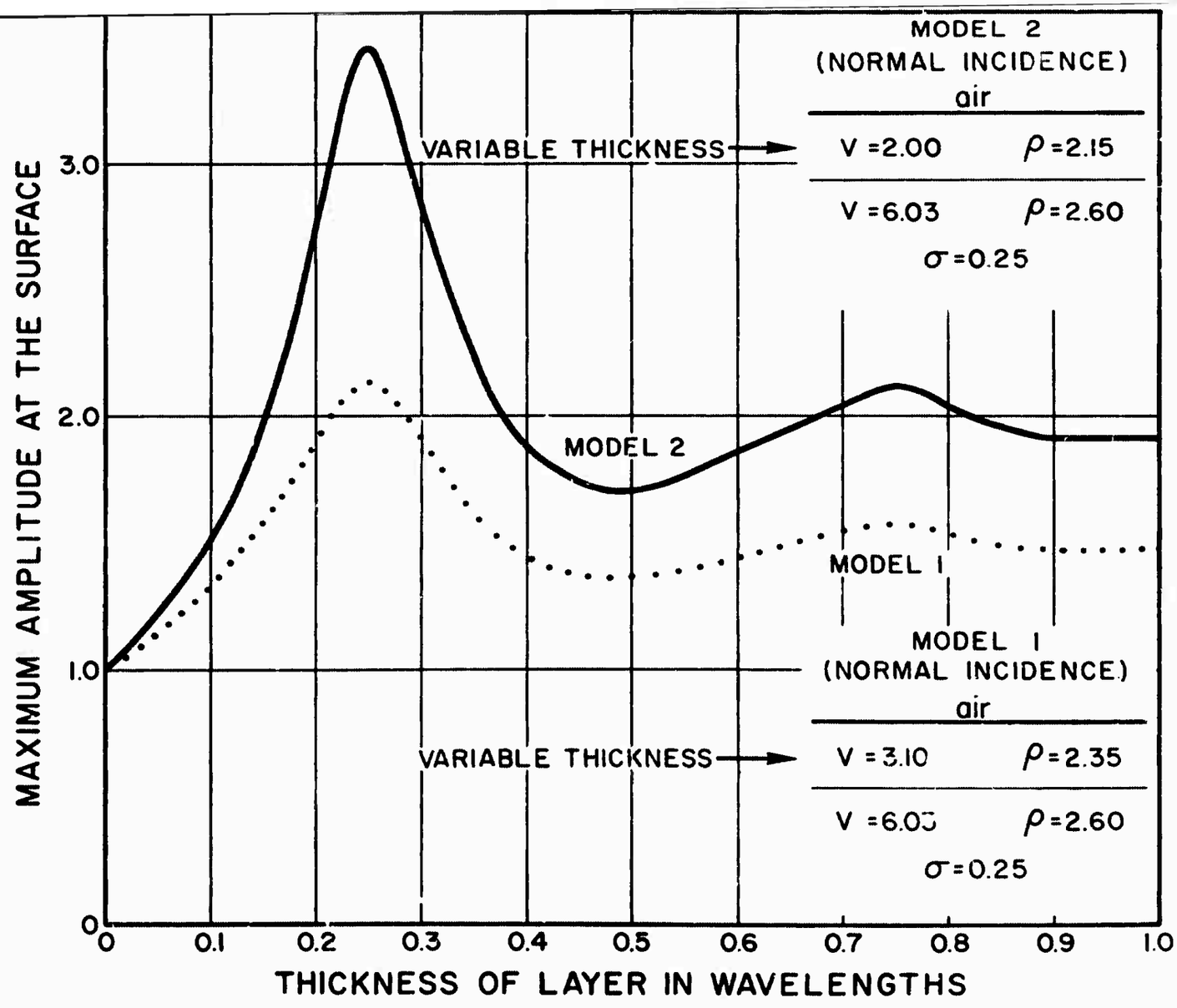

Signal Amplitude As A Function Of Thickness Of A Single Surface Layer

Figure 4

two limiting amplitudes is 1.30 which is equal to the square root of the inverse ratio of the corresponding acoustic impedances. The amplitude at resonance depends not only on the acoustic impedance but also on the reflection coefficient at the boundary. Thus, the resonant amplitude for Model 2 is 1.62 times the resonant amplitude for Model 1.

We experimented with several multi-layered models, including those with velocity inversions, but could find none that would give us appreciably larger amplitude effects. In conclusion, we have found that resonance is the most important factor in signal amplitude variation resulting from changes in near surface geology. To a lesser extent, the acoustic impedance of the surface rock is also important, a smaller acoustic impedance at the surface leading to a larger signal amplitude. As an order of magnitude, the signal amplitude may vary by a factor of three or four due to such causes in an idealized case; in practice, the variation is probably less.

In support of current interest in the performance at various sites, we used the above technique in predicting the comparative amplitudes of teleseismic signals received at a number of stations. These computations varied from the previous ones, however, in that the reference signal of unit amplitude was now incident on the Moho and not the top of the granite layer. In other respects, the present and previous computations were the same.

The models and results are shown in Figure 5. The models are based on as precise data as is available, plus, in some cases, some guidance from a knowledge of regional geology. In each of the models shown, the surface layer is sedimentary with a distinctly low velocity. In areas of igneous outcrops, such as those classically chosen as ideal seismometer sites, the models would be essentially as those shown without the sedimentary cover of velocities below 6 km per second. The thickness of the surface layer would be such that there would be insignificant resonance.

In each case, the amplitude of the signal incident on the Moho from below are considered to be unity. This means that, if there were no overlying crust, the amplitude would be

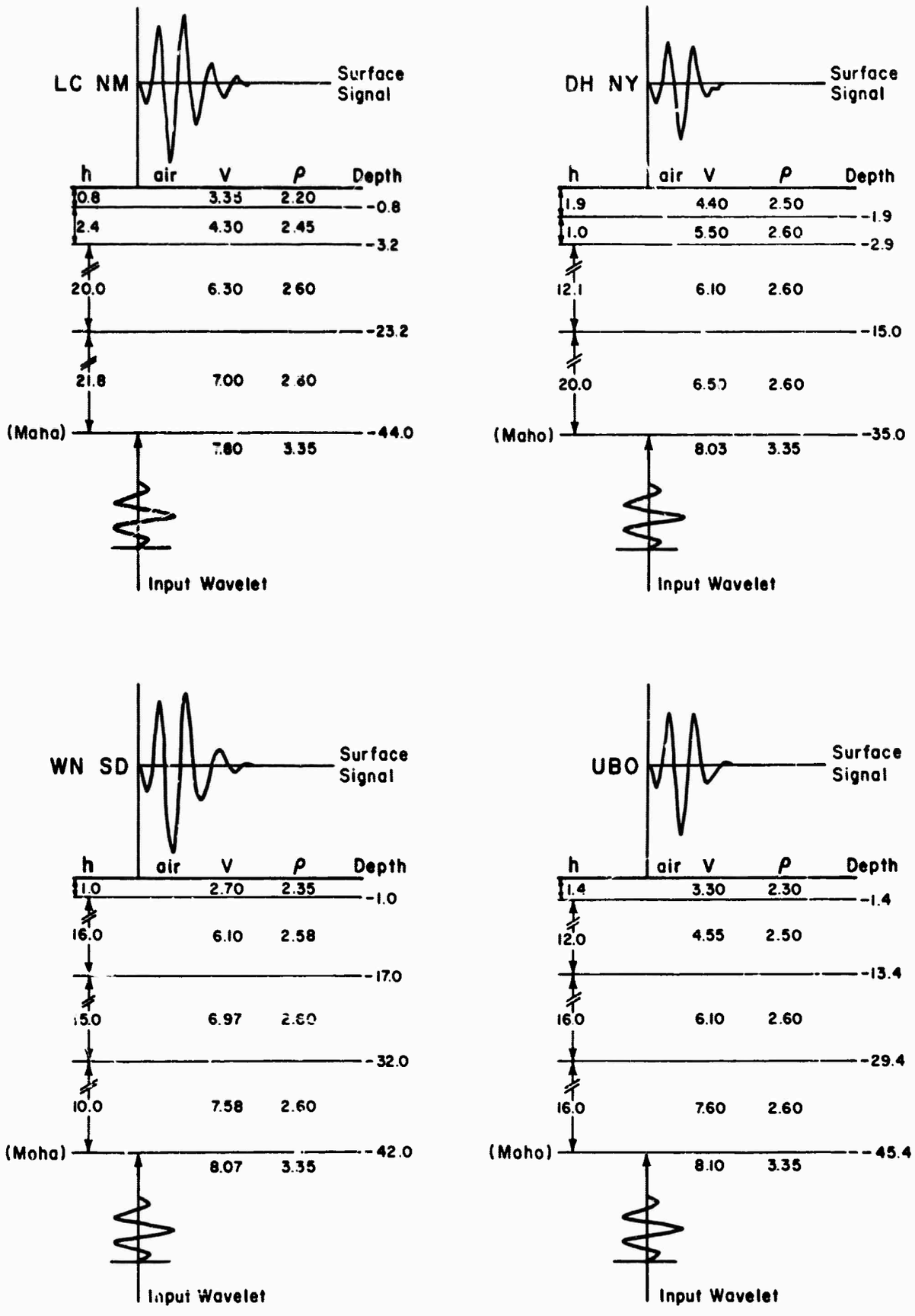

Earth Models and Typical Signals
as Received at Representative Stations.

Figure 5

2.0 at the free surface. The corresponding amplitudes at the four sites are 3.64 for Las Cruces, N. M. (LC NM), 2.40 for Delhi, N. Y. (DH NY), 3.88 for Winner, S. D. (WN SD), and 3.00 for Uinta Basin Observatory, Utah (UBO).

If there were no sedimentary layer and the surface layer were granite with a velocity of 6.03 and density 2.60, we used the acoustic impedances to get 2.64 as the corresponding amplitude. In computing this figure, we assumed no loss due to reflections at intermediate surfaces; thus the amplitude of 2.64 must be considered a reasonable approximation but still an upper limit. The thicknesses in this crust are such that we can disregard reverberations in considering the amplitude.

If we now wish to normalize the amplitudes in the sedimentary models to that in the shield model taken as unity, we have 1.38 for LC NM, 0.91 for DH NY, 1.47 for WN SD, and 1.14 for UBO.

In general, we can conclude that the signals amplitude in a region of sedimentary cover is higher than that in a shield region. However, in cases where the sedimentary sections contain limestones with high velocities, as at DH-NY, the signal can actually be lower than in the shield area.

D. Analysis of TFO Extended Array

During this reporting period various studies have been conducted to evaluate the use of large arrays, using the extended TFO array as the model. For example, we have computed the average correlations vs. distance and frequency for eight eleseismic signals and the preceding seismic noise.

The method of computing the correlations aligns the P-arrival, passes each trace through several narrow band filters, and computes the normalized zero-lag correlation coefficients between each filtered trace and a standard trace at TFSO. The results provide a measure of correlation vs. distance and frequency across the extended array.

The average correlations vs. distance with the variation in frequency as a parameter is shown in Figure 6 for both

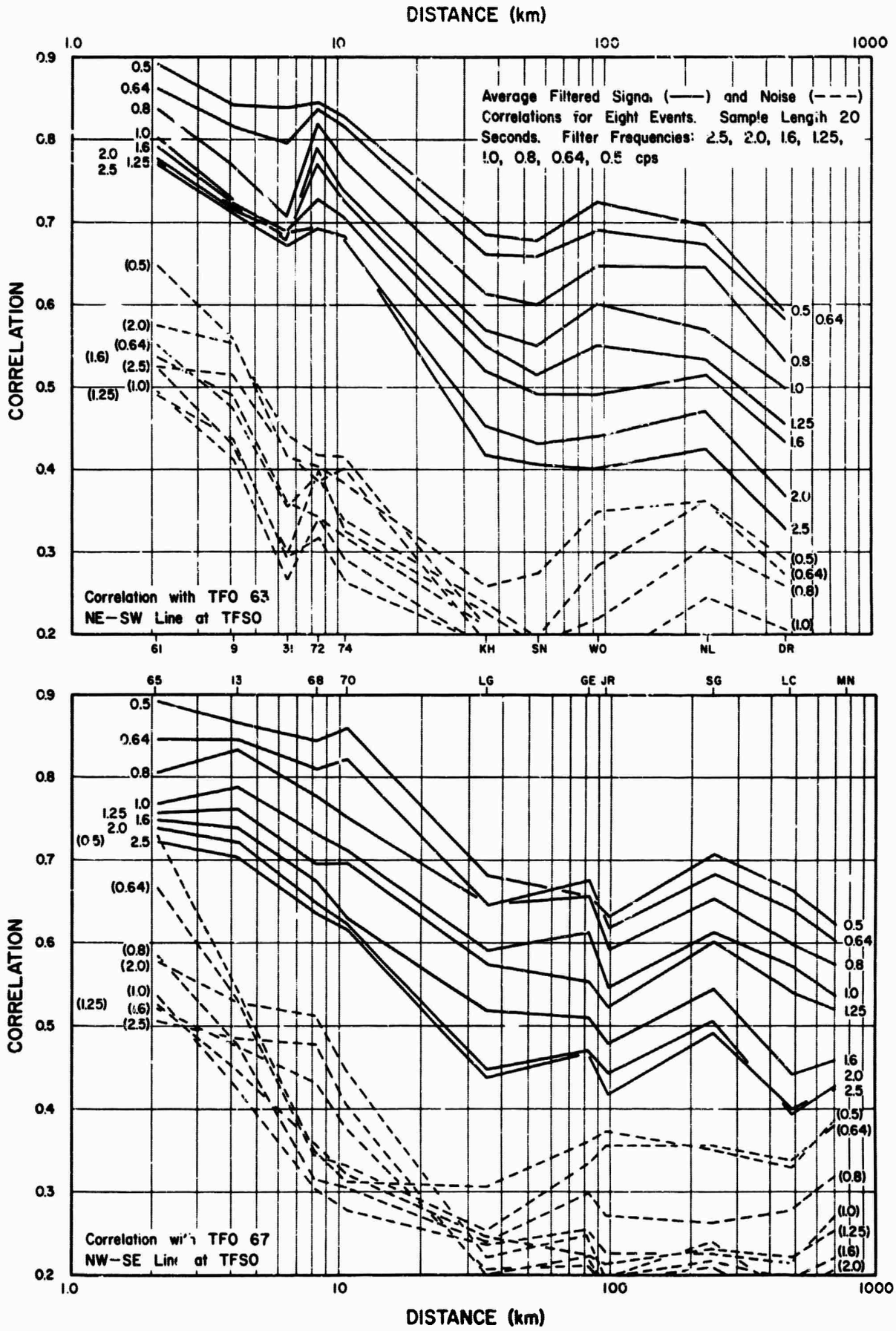

Signal And Noise Coherency Across Extended TFO Array

Figure 6

the NE-SW line and the NW-SE line. These results show that the signal correlations are higher than the noise correlations for almost all distances and frequencies. The noise correlations fall faster than the signal correlations especially for distances from 3 km to 100 km, similar to results for single events previously described. The correlations are systematically higher, the lower the frequency, for both signals and noise, as expected, since the array dimensions for these frequencies are larger in numbers of wavelengths.

All of the signal correlations show a decided drop between 11 km and 36 km. For distances less than 15 km, the correlations are between J-M seismometer outputs. For distances greater than 15 km, the correlations are between J-M and Benioff seismometer outputs. The two instruments differ in both phase and amplitude response and the difference is more marked at the higher frequencies. It is easy to show that both phase distortion and amplitude distortion will cause a lower correlation coefficient. We suspect that the large drop in correlations at this range is due to the change of instruments and that the signal correlations over the extended array are considerably higher than these results show. Since this data was analyzed, arrangements have been made at TFO to make it possible to repeat the study using all one type instrument.

We have also made some limited studies of travel time anomalies across the extended array. The events used were 18 Kurile Island earthquakes.

All travel time anomalies were measured relative to arrivals at MN NV, the nearest station in the extended array to the event epicenters. Relative, rather than absolute, anomalies were measured since P-onset times for some events at some stations were difficult to measure. On the other hand, picking a later characteristic feature of the P-phase (a particular large amplitude peak or trough) was fairly easy to measure and provided a measure of travel time intervals between stations.

The epicentral distances from MN NV ranged between 6461 km and 7564 km. The epicenters were all within $\pm$ 2.0^{o} of the same azimuth.

For the given epicenter, the Herrin-travel times for P-arrivals computed for all stations were subtracted from the observed arrival time of a particular feature of the P-wave. Then these observed travel times, minus Herrin travel time intervals at MN NV, were subtracted from the corresponding intervals at all other stations. The following Table 1 shows these intervals normalized to MN NV.

The travel time anomalies for 18 events from the same epicenter region showed that:

1. The extended array responds fairly consistently to these events. Most measured arrival times are within $\pm$ 0.2 seconds of the average.

2. Station anomalies are important. For example, NL AZ is roughly 0.6 seconds earlier than Herrin-travel time predictions.

3. Some of the scatter in the arrival times for these events is probably due to inaccuracies in the epicenter locations. Thus, the array may well respond more consistently than indicated by these results.

4. By taking account of station anomalies and expected travel times, the extended array can probably be velocity-filtered successfully, at least for events coming from the Kurile Islands.

In the future, this analysis will be applied to more events from the Kurile Islands and to events from other azimuths.

E. Automated Bulletin Process

Under AFTAC's direction, an Automated Bulletin Process (ABP) computer program was developed jointly by the SDL and the Geotechnical Corporation. The program associates seismic phase arrivals at a number of stations, with epicenters reported by the U. S. Coast and Geodetic Survey, and identifies up to 23 phases. The ABP is now being used to accelerate the preparation of the monthly earthquake bulletins of the five

	17 Jul	12 Aug	23 Jul	26 Jul	27 Jul	4 Aug	30 Jun *	13 Oct	7 Nov
MNNV									
SGAZ	+0.1	-0.2	+0.1	0.0	+0.1	-0.1	-0.1	0.0	-0.2
JRAZ		0.0	-0.1				-0.2	-0.1	-0.3
LGAZ	+0.2	-0.4	+0.1			0.0	-0.2	0.0	-0.1
DRCO	0.0	+0.1	+0.1	0.0	0.0	0.0	+0.1	-0.2	-0.1
NLAZ	-0.7	-0.9			-0.6	-0.8	-0.8	-0.6	-0.8
WOAZ	-0.2	-0.2	+0.2	-0.2		-0.1	-0.1		-0.3
KHAZ									
SNAZ	-0.1	-0.3	0.0	-0.2	-0.2	-0.1	-0.3	-0.1	-0.2
HPAZ	+0.5	+0.1	+0.5	+0.3	+0.3	-0.1		+0.4	+0.3
GEAZ	+0.2	-0.2	+0.2	-0.1	+0.1	0.0	0.0	0.0	+0.1
LCNM	-0.7		-0.3	-0.3	-0.5	-0.4	-0.7	-0.4	-0.6

	19 May	14 Sep	26 Aug	10 Aug	15 Oct	20 Nov	15 Jul	23 Oct	31 M
MNNV									
SGAZ	0.0	0.0	0.0	0.0	-0.1	0.0	-0.2	+0.1	-0.
JRAZ	-0.1	-0.1	-0.3		-0.2				0.
LGAZ			-0.1	0.0	+0.1	+0.2	-0.1	+0.3	0.
DRCO	0.0	-0.2	+0.2	0.0	+0.1	+0.1	-0.3	+0.2	0.
NLAZ	-0.6	-0.6	-0.5	-0.6	-0.6	-0.7		-0.3	
WOAZ	-0.1		-0.1	-0.1	-0.2	+0.1		+0.2	0.
KHAZ	+0.4								+0.
SNAZ	-0.2		-0.3	-0.2	-0.2		-0.2	+0.3	-0.
HRAZ			+0.3	+0.4	+0.3	+0.5	+0.4	+0.8	
GEAZ	0.0	+0.3	0.0		+0.1	+0.4	-0.1	+0.5	+0.
LCNM	-0.5	-0.5	-0.4	-0.4	-0.4	-0.2	-0.5	0.0	-0.

* pP Measured

TABLE 1

18 KURILE ISLANDS EARTHQUAKE 1964

RESIDUALS NORMALIZED TO MNNV

Nov
).2
).3
).1
).1
).8
).3
).2
).3
).1
).6

31 May
-0.1
0.0
0.0
0.0
0.0
+0.6
-0.1
+0.2
-0.2

VELA-UNIFORM seismological observatories published by the Geotechnical Corporation.

In terms of time and manpower requirements, most of the work of preparing the earthquake bulletins involves:

1. Measurement of arrival times, amplitude, and period, preliminary phase identification based on signal character, and card-punching these data for each station. Analysts may record from 300 to 2000 events per month at each station, depending upon the station, time of year, and seismic activity for a given month.

2. Association of phase arrivals with hypocenters reported in the U. S. Coast & Geodetic Survey (USC&GS) Preliminary Determination of Epicenter (PDE) cards, identification of phases, merging of associated and unassociated events, computation of azimuth, distance, magnitude, and ground displacement, and finally, combination of all data from the five observatories into a form suitable for publication.

The ABP was designed to automate the latter task.

The ABP has been written in three parts (Figure 7). These three parts can be combined into one program but are usually run independently.

Part I computes the predicted arrival times of 23 seismic phases from known hypocenters at each of any number of stations. Part II identifies, associates, and merges the observed arrivals at each station with the hypocenters input to Part I. Part III rearranges the associated and unassociated phases into bulletin format and, by incorporating a program written by J. G. Swanson of the Geotechnical Corporation, computes ground displacement and magnitude. Part III also computes distances for local and near regional events based on tables of phase intervals vs. distance. Finally, Part III writes the entire bulletin on

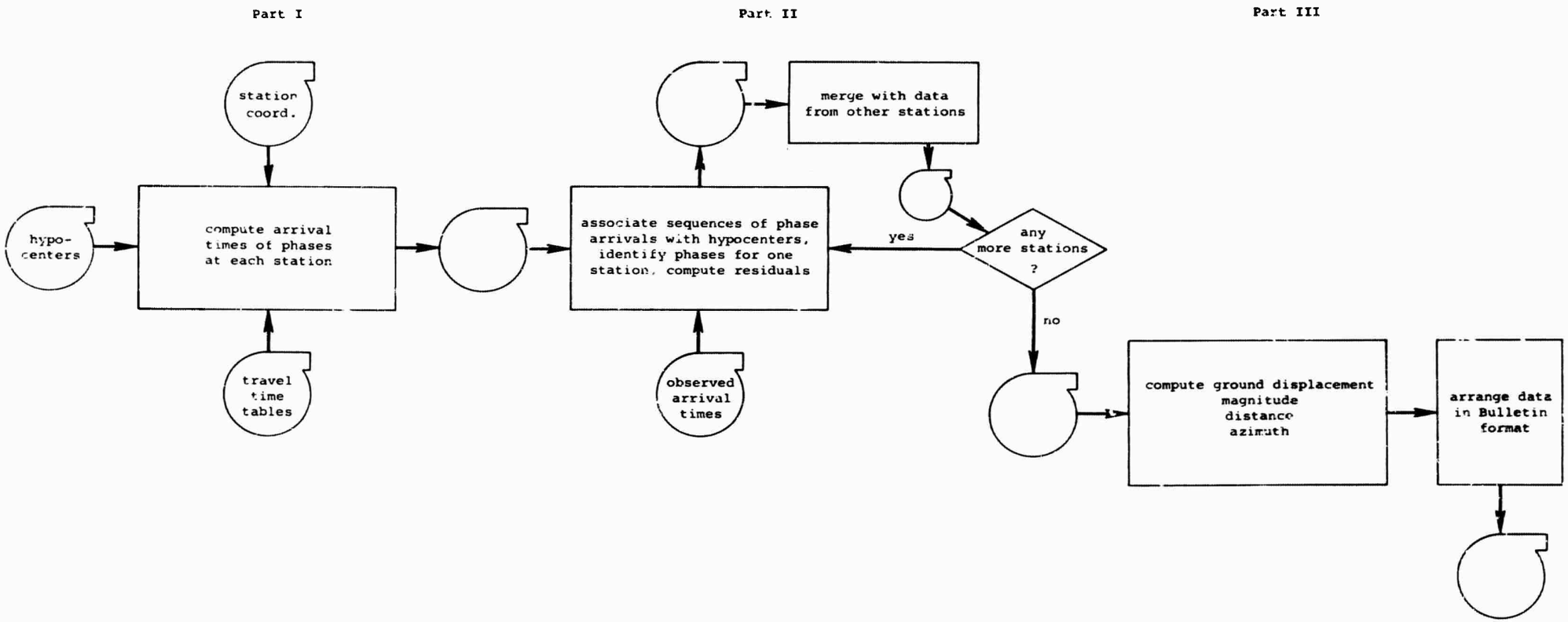

Schematic Routine On Which The Automatic Bulletin Processing Is Based

Figure 7

magnetic tape in the card inage format from which it is published.

Often, an analyst identifies a phase and determines the azimuth and distance from a hypocenter to his station from the character of the seismogram or by using other criteria. Subjective criteria are difficult to translate into specifications for a computer program; the analyst is encouraged to record this data, even though he has no hypocentral information, because in the following cases the analyst's interpretation prevails over the ABP decision:

1. For events not associated with hypocenters reported on the PDE cards, the analyst's identifications are used.

2. If the phase arrival is part of a sequence that has been identified as a local (L), or near regional (N) event by the analyst, and if the arrival falls within the expected arrival time window of a located teleseismic (T), or regional (R) event, then the event is left unassociated and the station analyst's phase identifications are used.

3. The ABP does not attempt to identify Love or Rayleigh phases. These phases are identified by the station analyst.

In all other cases, the ABP overrides or blanks out the analyst's identification. However, the choice of which of the analyst's phase identifications the program will supercede, can be specified.

Allowable residuals for phase identification are based on statistical distribution of time residuals observed for each of the 23 phases which ABP attempts to identify. A digital magnetic tape was prepared containing focal depth, station-to-epicenter distance, station name, and phase arrival time for all identified phases from 1613 known hypocenters recorded at BMSO, CPSO, TFSO, UBSO, and WMSO during April, May, June, and October 1963.

From these data, the 23 most commonly recorded phases were selected, the mean arrival time residuals were determined for those phases, and a "maximum allowable" residual value, was established for each phase, based on commonly observed frequencies of the phase. The reamining phases such as PcS, PSS, SSP, etc., represent less than one per cent of the total number of phases identified by the analysts.

Any residuals which fell outside this "maximum allowable" value were assumed to be the result of inaccuracy of the PDE data, data transcription errors, or questionable phase identifications, and were not used in the determination of the mean residual for that phase. All association windows are approximately equivalent to the mean arrival time residual plus or minus twice the standard deviation, except in the cases of P and PKP where the windows are equivalent to the mean residuals plus or minus three times the standard deviation.

The ABP takes six hours on the CDC 1604 to process one month's data for the five VELA observatories. Each station's arrivals are processed independently and merged with data already processed for other stations. Under this system, a bulletin can be generated for any number of stations, or the program can be restarted after a one, two, or three station bulletin has been written on magnetic tape for a given month.

To date, the ABP has been run for the September, October, November, and December 1964 bulletins.

Bulletin data from February 1963 through December 1964 has been written on magnetic tape in a compact format to facilitate retrieval. A set of programs has been written to process the Bulletin data, summarizing the frequency of occurrance of each phase at each observatory as a function of earthquake magnitude, depth, and distance.

F. Shot and Earthquake Analyses

1. SALMON

SALMON, the first shot of the DRIBBLE series, was detonated at the Tatum Salt Dome near Hattiesburg, Mississippi, on 22 October 1964. Thirty-eight stations recorded short-period signals and 20 stations recorded long-period signals.

A Mexican earthquake, occurring approximately 4 minutes after the SALMON explosion, possibly interfered with western U. S. stations recording the surface waves from SALMON. The average magnitude for SALMON was 4.58, and two stations, Eutaw, Alabama and Jena, Louisiana, showed compressional first motion as defined by the TWG II First Motion Criteria. The travel-time residuals from the Pn and P phase corresponded favorably with those derived from the GNOME event and showed that, generally, the apparent upper mantle velocities are substantially higher to the east and north than to the west towards the Nevada Test Site. The most distant station that recorded SALMON was La Paz, Bolivia, at a distance of 5704 kilometers.

2. Texas-Louisiana Earthquake (24 April 1964)

The average magnitude was 4.36, and short-period signals were recorded by 30 stations; no long-period signals were recorded due to interference from a larger magnitude (6.3) New Guinea earthquake. Two stations Jena, Louisiana and Grapevine, Texas, showed rarefactional first motion as defined by the TWG II First Motion Criteria.

3. West Virginia Earthquake (25 November 1964)

The average magnitude was 3.95, and short-period signals were recorded by 27 stations; the station at Beckley, West Virginia recorded a long-period surface wave, identified as a high frequency sedimentary Rayleigh wave. None of the stations showed compressional or rarefactional first motion as defined by TWG II First Motion Criteria.

4. Seismic Waves From the SS Village Explosion

This was a chemical explosion at approximately 7,000 feet underwater which took place aboard a ship being sunk in the Atlantic Ocean off the coast of New Jersey and Delaware on 17 September 1964. The average magnitude was 4.45, and short-period signals were recorded by 30 stations; no stations recorded any long-period data. Four stations, Delhi, New York, Beckley, West Virginia, Houlton, Maine, and Jerome, Arizona, showed compressional first motion and one station, Berlin, Pennsylvania, showed rarefactional first motion, as defined by the TWGII First Motion Criteria.

The character of the records was definitely influenced by multiple water reflections which appeared to repeat a number of times. Although the time intervals between peak amplitudes appeared about constant, the onsets of the individual reflections were difficult to pick. It was also noted that the character of the multiples varied from station to station indicating possible receiver and path effects.

In Figure 8, three typical seismograms are shown; time intervals of the Pn and P multiples as determined are consistant with those from many other records. These are indicated by the solid lines. The spacing of the multiples (2.6 seconds) is dependent on the thickness of the water layer. With the hypothetical shot position as shown, the shot should produce another set of pP multiples equal in amplitudes to the corresponding P multiple amplitudes. These are not readily apparent; so it is probable the shot occurred at the liquid-solid interface. However, the absence of a well defined pP multiple could also be explained by distortion of the wave form caused by the time lag and phase relationships of the multiple with some other phase.

G. REMODE (Rectilinear Motion Detection)

Studies in rectilinear motion detection at SDL evolved from a long series of experiments related to the use of the analog computer in processing seismograms recorded on magnetic tape in analog form. These studies have led to a class of operators which we have named **REMODE**, standing for Rectilinear Motion Detection. Our **REMODE** repertoire contains both analog and digital programs, both of which we are actively testing and modifying as better techniques are discovered.

Early studies of this series included the sum of the squares of three-component seismograms on which we have already reported. Later studies included matched filters.

A signal waveform which is reasonably constant from place to place for a given type of event such as an explosion would make possible the use of a matched filter to enhance signal detection in an automatic system. The purpose of this study was two-fold:

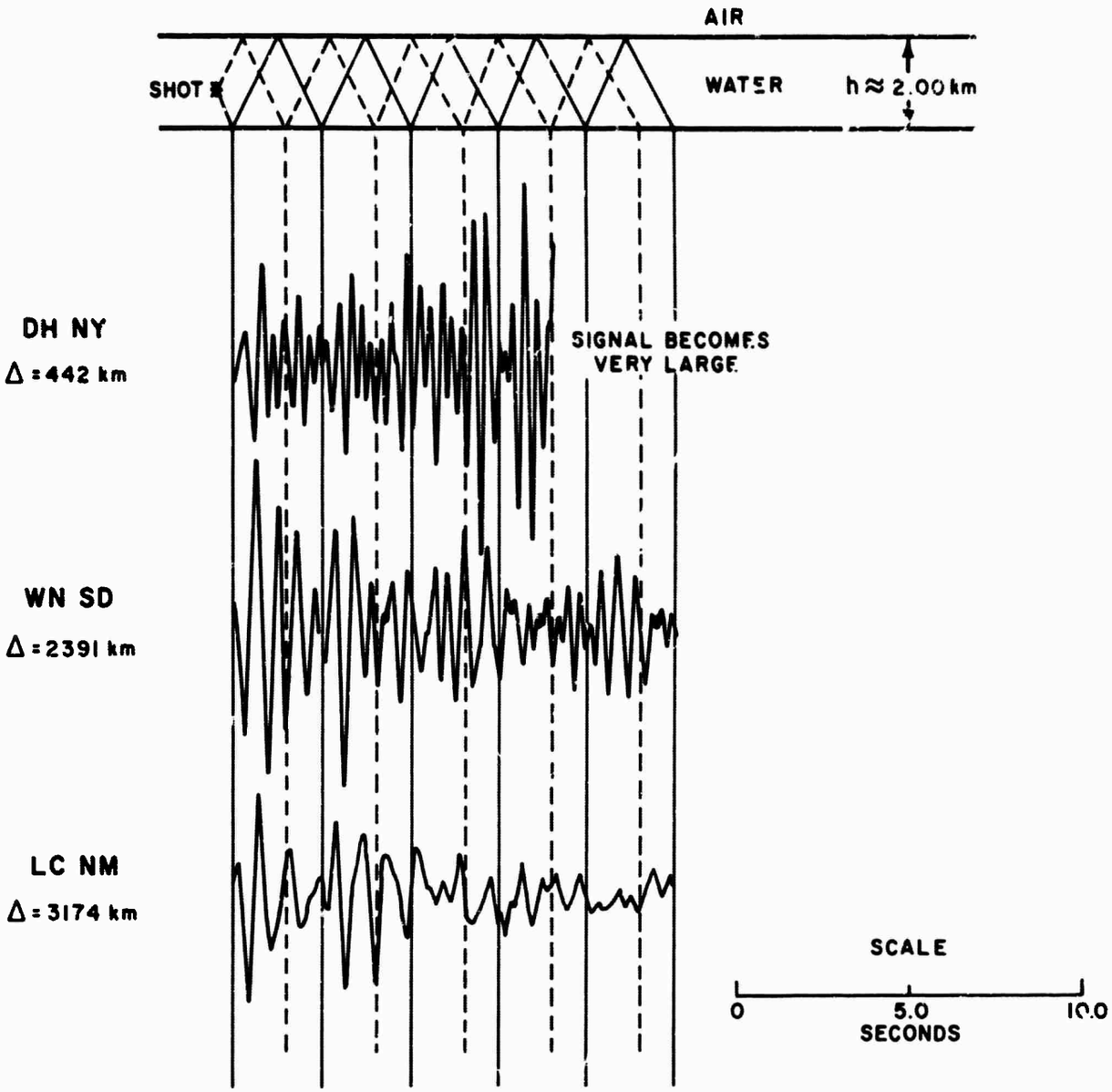

Multiples in a Water Layer

Figure 8

1. To determine to what extent signal waveforms from explosions are consistent; and,

2. To determine whether a matched filter successfully enhances the determination of first motion.

Similarities of waveforms have been determined for two Russian and two Algerian events as recorded at BL WV, DR CO, and LC NM. The waveforms were presented as Laguerre approximations (20 coefficients) to the initial pulse. Averages for the signals from each region were also made. Comparison of the waveforms showed considerable similarity but also some disadvantages of this method of approximation. For example, many of the individual waveforms displayed a high frequency noise introduced by the approximation.

The average signal for two evnets analyzed was used as a matched filter to process seismograms from three events as recorded at BL WV, DR CO, and LC NM. In each case, the third seismogram was noisier than the two for which the signal approximations were derived.

The original data traces were processed through the matched filter formed from the average signal. The data traces were then processed through the quadrature filter (same amplitude response as the matched filter but with a 90^{o} phase shift). If we square each of the corresponding filtered traces and add, the resulting correlation traces display sharp maxima related to the original signals as shown in Figure 9. The time origin chosen for the average waveform is such that the sharp maxima on the final traces indicate the onset of the signal. The following table shows the precision found for these events and stations.

Results Of Squaring And Summing The Direct And Quadratured Matched Filter Outputs

Figure 9

TRAVEL TIMES DETERMINED BY MATCHED FILTER TECHNIQUE

FOR SAHARAN EVENTS

DATE		BL WV	DR CO	LC NM
1 May 1962	Detector Time	10:11:31.2	10:13:12.2	10:13:21.0
	Origin Time	10:00:00.3	10:00:00.3	10:00:00.3
	Travel Time	11:30.9	13:11.9	13:20.7
18 March 1963	Detector Time	10:13:31.2	10:15:12.4	10:15:21.4
	Origin Time	10:02:00.5	10:02:00.5	10:02:00.5
	Travel Time	11:30.7	13:11.9	13:20.9
20 October 1963	Detector Time	13:11:30.9	13:13:12.0	13:13:20.8
	Origin Time	13:00:00.1	13:00:00.1	13:00:00.1
	Travel Time	11:30.8	13:11.9	13:20.7

In the study of matched filters it was learned that there was a danger of false alarms which might be overcome or reduced by some sort of filtering. Frequency filtering will not satisfy this requirement because the false alarms generally have their origins in the frequency band of the matched filter. As a solution, we have considered coherency filtering in several forms. Further, in order to better understand the processes being studied, we have examined coherency filtering of very narrow passbands.

We first made up pairs of synthetic seismograms by mixing a given signal with different samples of noise.

Each seismogram trace is decomposed into seven narrow-band components:

$$Z_n(t) = Z(t)*W_n(t) \text{ and } R_n(t) = R(t)*W_n(t)$$

where n varies from one to seven. The filters in this experiment were constructed with Q = 5, and the center frequencies were 0.64, 0.8, 1, 1.25, 1.6, and 2 cps.

For any given frequency component, the simulated vertical component was correlated with the simulated horizontal component to get the correlation function:

$$C_n(t) = \frac{\overline{Z_n(t) \cdot R_n(t)}}{\left[\overline{Z_n^2(t)} \cdot \overline{R_n^2(t)}\right]^{\frac{1}{2}}}$$

A gain function $G_n(t)$ of the form $e^{-C_n(t)}$ was constructed and made to operate on the vertical trace. The final output was composed by summing the seven components

$$Z^*(t) = \sum_{n=1}^{7} G_n(t)\, Z_n(t)$$

Similar correlations were made basing the correlation criteria and gain control G' on the comparative amplitudes one would expect to get on the two components for a given angle of emergence or azimuth. We also performed cross-correlation between traces from adjacent frequency bands and used the resulting function as a gain control on one of the traces. The actual cross-correlation function used for a given frequency band was the average of the correlations between the trace for that band and the traces for adjacent bands on either side (where both exist):

$$C'_n(t) = \frac{1}{2}\left\{\frac{\overline{Z^*_n(t) \cdot Z^*_{n-1}(t)}}{\left[\overline{Z^{*2}_n(t)} \cdot \overline{Z^{*2}_{n-1}(t)}\right]^{\frac{1}{2}}} + \frac{\overline{Z^*_n(t) \cdot Z^*_{n+1}(t)}}{\left[\overline{Z^{*2}_n(t)} \cdot \overline{Z^{*2}_{n+1}(t)}\right]^{\frac{1}{2}}}\right\}$$

and the corresponding gain control $G'_n(t)$ was of the form $e^{-C_n(t)}$.

An example of the output for a single frequency band is shown in column B of Figure 10; the band shown is the center band of the seven used and is that of the apparent frequency of the input signal. In column C of the same figure are shown

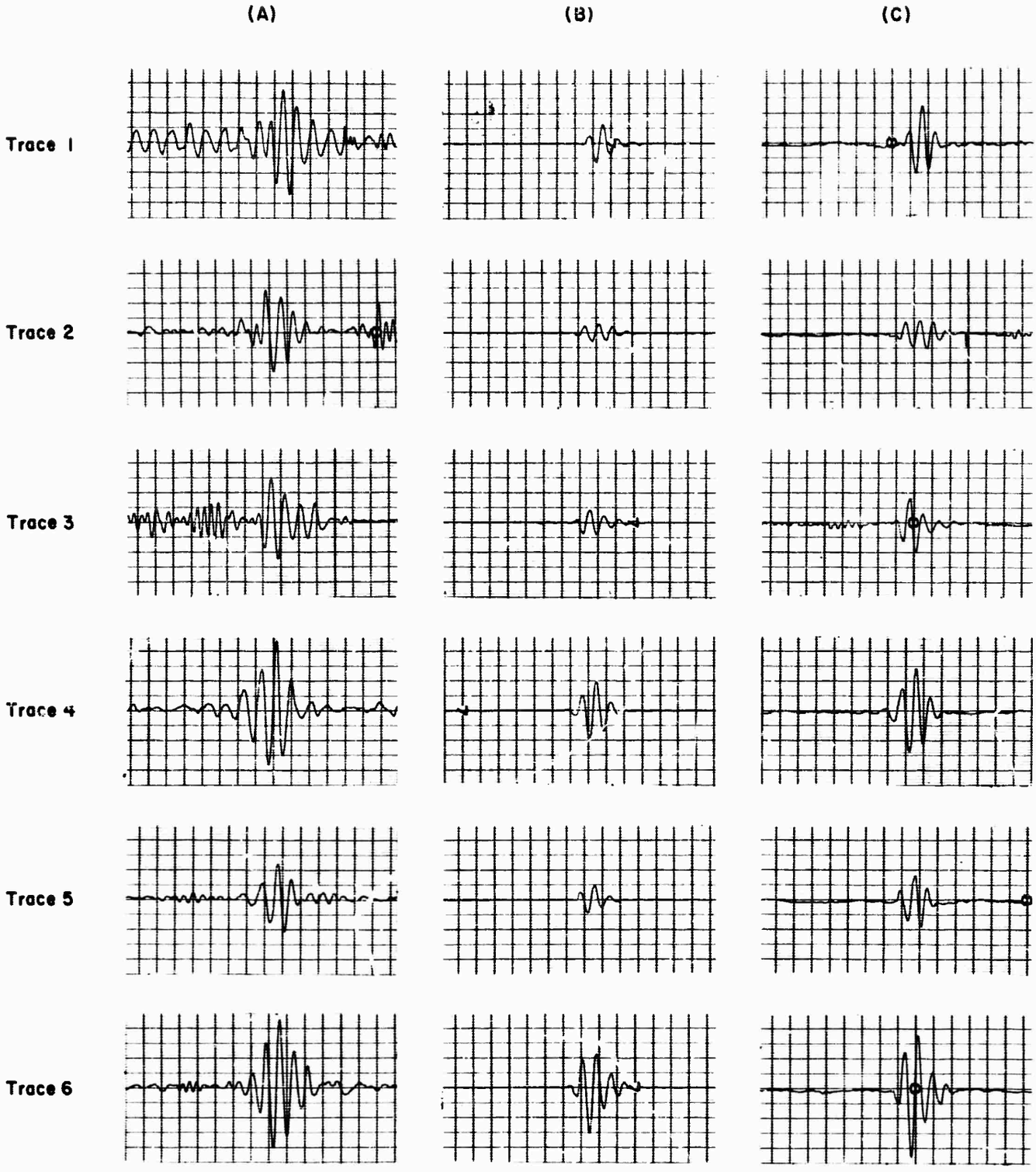

Examples of Synthetic Records After Correlation Filtering Preceeded by: (A) Directional Filtering; (B) Directional Filtering and Subsequent Correlation Between Adjacent Frequency Bands (Center Band Only); and (C) the Same as (B) with all Frequency Bands Summed After Filtering

Figure 10

examples of the final output defined by

$$Z^{**}(t) = \sum_{n=1}^{7} G''_n(t)\, G_n(t) G'_n(t) Z_n(t)$$

We now consider the basis of REMODE to lie in the fact that the onset of P-wave signals tends to be in phase on both the horizontal and vertical components of seismograms; conversely, seismic noise tends to be randomly in or out of phase on the horizontal and vertical components. This relationship, as well as others, is useful as a basis for extraction of seismic signals from noise. Specifically, for example, a raypath corresponding to a body wave phase initially emerges at the receiver at a unique angle depending largely on the distance from the source. Such an arrival is expected to produce similar particle motion on the radial and vertical components. On the other hand, the horizontal and vertical components of seismic noise are often observed to have very little similarity in waveform; the noise field, consisting of many vibrational modes of different orbit and direction of propagation, can be expected to produce rapidly changing and largely uncorrelated waveforms on both the horizontal and vertical components.

A method is drawn from electrical engineering to determine the operator which extracts a least squares estimate of a common waveform present in two time series. For weak body waves, the application of the extraction operator improves the signal-to-noise ratio, and isolates phases which cannot otherwise be detected with a narrow band-pass filter. Strong body wave phases, which would otherwise be obscured by signal generated noise, are also isolated.

We distinguish between two classes of operators: zero lag correlation coefficients are labelled "scalar parameters" and correlation functions involving the convolution integral are labelled "functional parameters". In general, where as prior work in this field has been restricted to use of the zero lag correlation coefficients, we recommend use of the more comprehensive correlation functions. In particular, we have found the best results in using as a gain control the

even part of the cross-correlation function between the two traces in question.

Figure 11 illustrates the efficiency of the even part of the correlation function in extracting signal from Gaussian noise.

We have mixed a given signal with different random noise samples at a peak signal-to-noise ratio of one. Gaussian noise was obtained from a random noise generator passed through a linear filter which simulates the Benioff system response.

The processed seismograms are shown. In each case, the operator number indicates the trace on which the filtering was performed. It is evident that a considerable improvement has been attained in the signal-to-noise ratio, at the same time maintaining the signal shape reasonably well.

By contrast, the results of band-pass filtering on the same synthetic records are distinctly inferior and one would not expect to improve even after considerable effort to find the optimum band-pass filter.

We feel that small arrays of three-component seismometers are the most suitable for REMODE filtering. As a preliminary trial we present an example of REMODE filtering on the 7-element array at Oslo, Norway (Figure 12). It can be seen that an almost unpickable seismogram has been converted to a useful record by the REMODE operation. In this case, since there was only one three-component instrument at the site, the F vertical seismograms were velocity filtered and summed before REMODE filtering.

The actual shape of the pulse passed by the filter is likely to be quite distorted, especially when the S/N ratio is low, since, in addition to distortions introduced by the filter itself, the sum of the noise and signal is admitted, inasmuch as the filter acts somewhat like a gate. Hence, this filter provides information on the time of first motion and the interval of rectilinearity for a phase but little highly reliable information on the pulse shape. Indeed one might expect the signal as admitted by a REMODE filter to

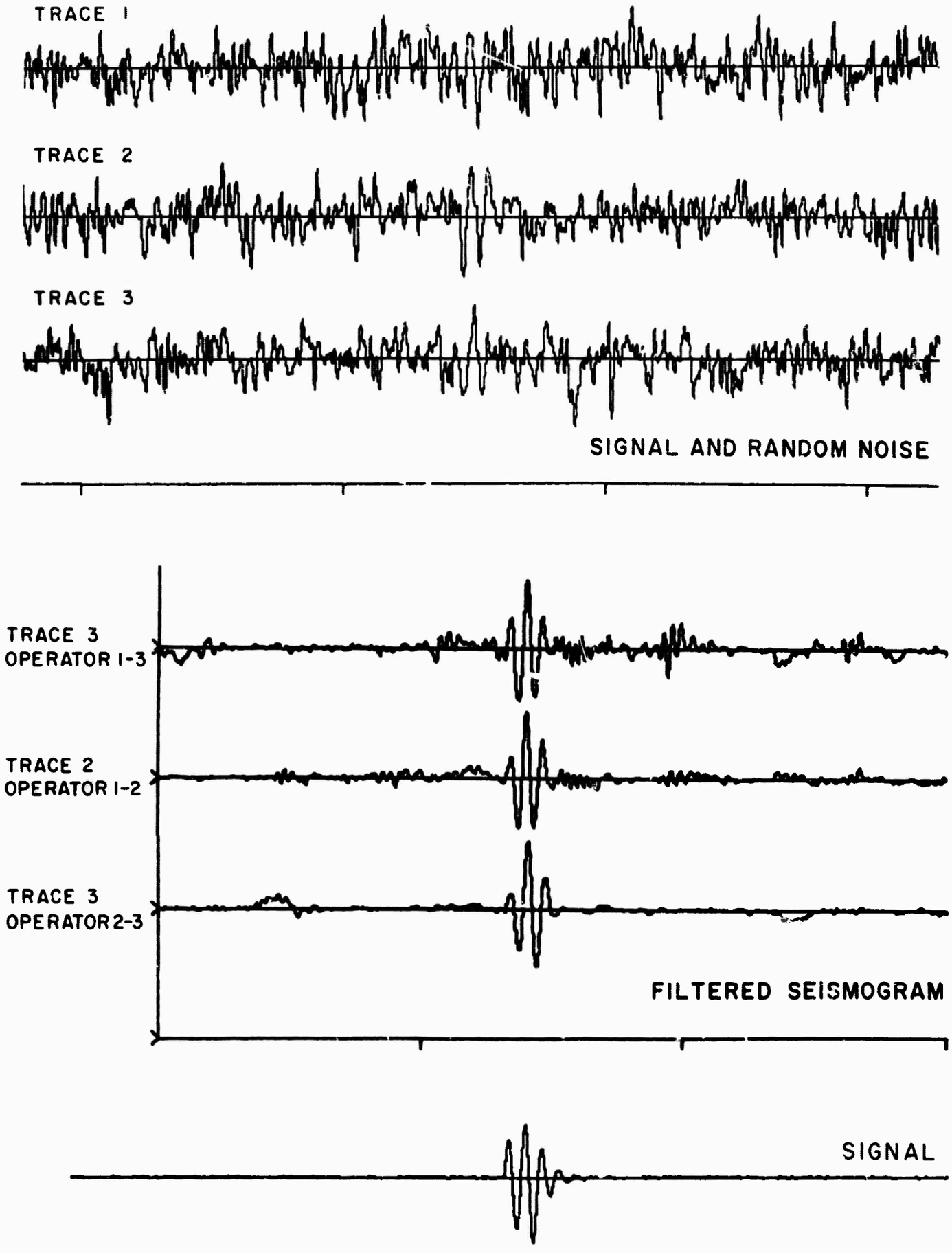

Examples Of The REMODE Operation On Signals Buried In Gaussian Noise

Figure 11

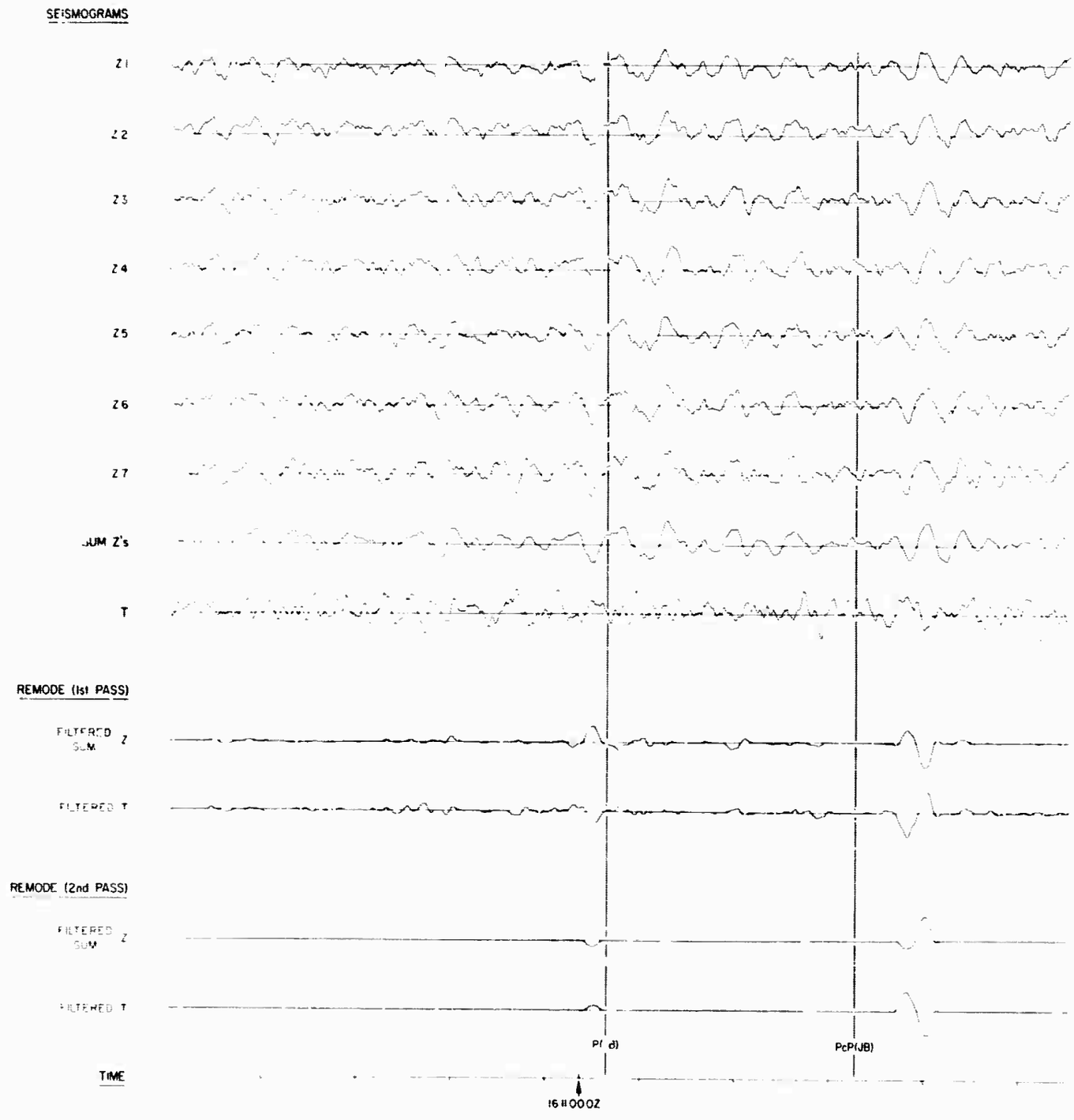

REMODE Array Processed Seismograms for OSLO, NORWAY,
Δ = 7565 Km, SALMON Event

Figure 12

look much like a section of the noise when the S/N ratio is low. This appears to be the case with the REMODE trace for the Oslo array, although the true shape of the pulse is itself unknown.

H. Supplemental Analysis of SALMON Data

A rectilinear motion detection (REMODE) technique has been used to isolate arrivals from the SALMON event at teleseismic distances in several cases where the signal-to-noise ratio was low and visual methods or the ordinary array processing procedures failed. The essential aspects of array and single station REMODE processors currently in use were outlined and examples from the SALMON event were processed. The phase isolation capability of the processor seemed most promising and was fully exploited in the analysis of the SALMON data. In particular, P-wave travel time data was obtained from the processed traces along three azimuths from the SALMON site. The travel time curves obtained showed reasonably well-defined multiple branches. An inversion method giving the velocity structure appropriate to these data was briefly described, and the structures obtained from the SALMON data were discussed. Radiation patterns appropriate to the primary travel time branch for the P-wave were obtained for various frequencies, and these were interpreted in terms of an ideally symmetric and purely compressional source. Comparisons were also made to theoretically derived radiation patterns for explosive sources with associated tectonic energy release.

The surface wave dispersion along the three profiles from the SALMON site has been measured and an inversion method for this data was discussed. Velocity structures appropriate to the surface wave data were described and compared to the body wave structures. Rayleigh wave radiation patterns were also obtained and interpreted in terms of a compressional source.

A few general observations concerning the source and the associated seismic field can be made from a preliminary analysis of the signal from this event.

Fundamental mode Rayleigh waves were identified at 21 LRSM stations, in the period range 8 to 40 sec., out to

about 2500 km. Higher mode Rayleigh waves were observed to distances of 3000 km on the continent and at nearly every operative LRSM station. P phases were detected at all but one or two continental LRSM stations and at La Paz, Bolivia, at a distance of 5704 km. The long period Rayleigh wave excitation was not very great, as might be expected, and the signal-to-noise ratio was generally quite low, except at the closest pair of staions. In addition, the occurrence of an earthquake in Mexico either complicated or completely obliterated the Rayleigh waves at some of the western stations. Consequently, the analysis of surface wave radiation was limited to 14 stations. On the other hand, the quality of the short period data was uniformly good and uncomplicated by other events, so that all LRSM stations (40) were used in the body wave analysis.

As with the GNOME event, no Love wave radiation was observed. This is in contrast to most of the NTS shots, for example, SHOAL and BILBY, which produce SH surface waves of this type. One may note that the presence of Love waves would be expected if tectonic energy release occurred. While NTS is in a tectonically active area, and the medium would normally be prestressed, SALMON and GNOME were in salt and would not support even a modest prestress field. Thus, the lack of SH radiation from SALMON and GNOME would be consistent with the presence of such radiation from NTS events if tectonic release were involved. The observations are still, however, open to other interpretations.

P-wave arrivals along the NW profile were approximately the same as the J-B times, while on the N profile they were 4 to 5 seconds earlier than the J-B times. These observations were in general agreement with those from GNOME.

Figure 13 shows two especially good examples of the signal-to-noise enhancement and phase isolation capability of the filter. The traces shown correspond to single LRSM stations, so that the array processor degenerates to a simple double application of the REMODE filter in this case. The event shown is SALMON, and the stations are in the 20° distance range and, as might be expected, several clear P arrivals have been isolated, presumably corresponding to an inverse branch or multiple branches of the travel time curve. As was previously pointed out, these

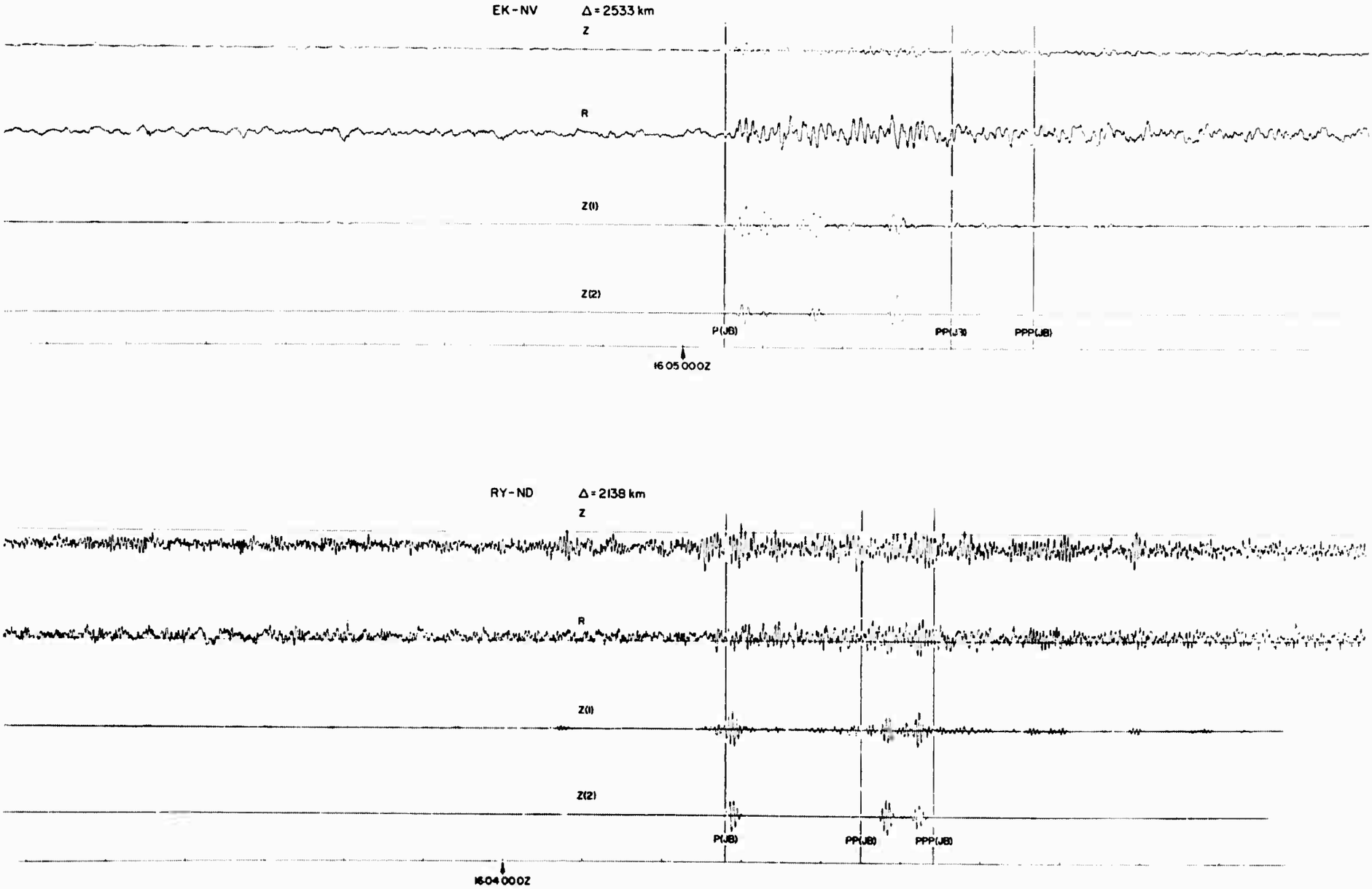

REMODE Seismograms for SALMON (EK-NV and RY-ND)

Figure 13

filtered traces should correspond, for a properly designed REMODE filter, to the nearly rectilinear first motions of the individual phases.

Of the stations processed in this study, roughly 30 percent gave REMODE outputs with S/N enhancement and phase isolation comparable to the examples shown.

The most common failing in the remaining processed records, aside from occasional reductions in the overall signal to noise enhancement feature of the process, was the absence of a clearly isolated P_n arrival in the zone where the S/N ratio for P_n is low. While this apparent lack of sensitivity may be due to the manner of data presentation (i.e. the scaling of the plotted filter output), it most likely indicates a threshold of S/N for detectibility, with this particular filter at least. The precise threshold limits are observed to vary from location to location however, so that one must conclude that the character of the noise and signal, but especially of the noise, determines to a great extent the sensitivity of the filter to small amplitude rectilinear signals.

In examining signal spectra as a function of distance, it is clear that the maximum spectral amplitude for P shifts to longer periods with increasing distance, due to the roughly linear increase in attenuation with frequency. The observed attenuation will, of course, be affected by the variation of the dissipation function Q with depth in the earth[8] so that the attenuation will be dependent on the actual minimum time path followed by the phase. This effect would be of second order, however, compared to the much larger amplitude affects associated with the velocity variations with depth, particularly with velocity reversals and rapid or discontinuous changes in velocity.

Thus, the observed spectra would not be expected to fall off uniformly with distance in the range where the minimum time paths would be strongly affected by the velocity variations in the upper mantle of the earth. Indeed, strong and rapid variations with distance would be expected in view of the likelihood of large gradients in the velocity variation with depth and the existence of the low velocity zone in the upper mantle.

[8] Anderson, D. L. and Archambeau, C. B., The Anelasticity of the Earth: J. Geoph. Res., vol. 69, pp. 2071-2084, 1964.

A comparison of spectral amplitude with distance at particular frequencies is given in Figure 14. The anomalous behavior only suggested by the individual spectra is now quite apparent. The essential aspects of the amplitude-distance variation obtained and illustrated in this figure have been observed many times before by other investigators, and in particular, for events observed along a profile of stations in this same region[9]. The spectral detail in the present case is perhaps somewhat greater than has been available before, so that a correspondingly more detailed interpretation will be advanced.

The spectra will be interpreted together with the observed travel time curves. However, viewed independently, they show a fairly rapid fall-off with distance out to approximately 1250 kilometers. The rather gradual increase in amplitude, beginning at this point and reaching an apparent maximum at 1800 to 1900 kilometers, probably indicates a first arrival P-phase different from P_n. A decrease in amplitude at around 2000 km, followed by a second peak in the spectrum again probably indicates a second P-phase.

This rather superficial interpretation has been checked with the travel time observations for evidence of changes in the first arrival curve slope as well as for the existence of multiplicities or cusps in the curves accounting for the amplitude maxima.

Figure 15 shows the travel time versus distance data for all profiles combined. The data shown correspond to first arrival phases and all phases within 20 seconds of the first arrival at a given distance, with the exception of those identified as PP and PPP. At the greater distances some of the later arrivals are shown since they were often of large amplitude and may be related to mantle velocity variations which manifest themselves in the first arrival curves at somewhat greater distances than those considered in the present study. The travel time observations obtained for PP and PPP from the REMODE processed time series have the expected character as functions of distance and serve, in part, to increase the confidence with which one may interpret the travel times for other phases, particularly the P_n and P travel times.

The solid circles in the figures indicate large amplitudes

[9] e.g. Romney, C., Brooks, B. G., Mansfield, R. H., Carder, D. S., Jordan, J. N., and Gordon, D. W., Travel Times and Amplitudes of Principle Body Phases Recorded From Gnome: Bull.Seis. Soc. Amer., vol. 52, pp. 1057-1074, 1962.

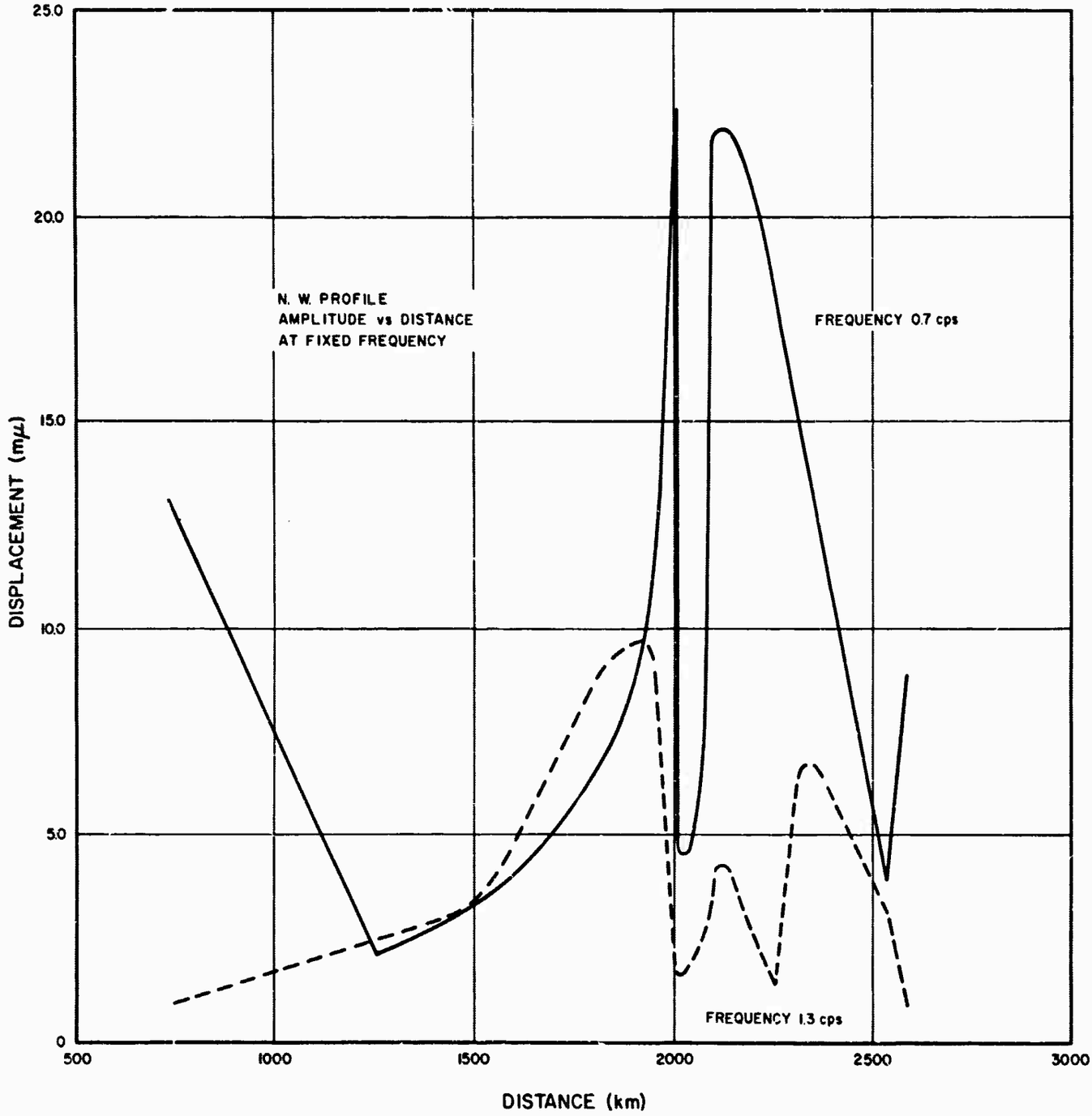

Amplitude versus Distance at Fixed Frequencies, N. W. Profile

Figure 14

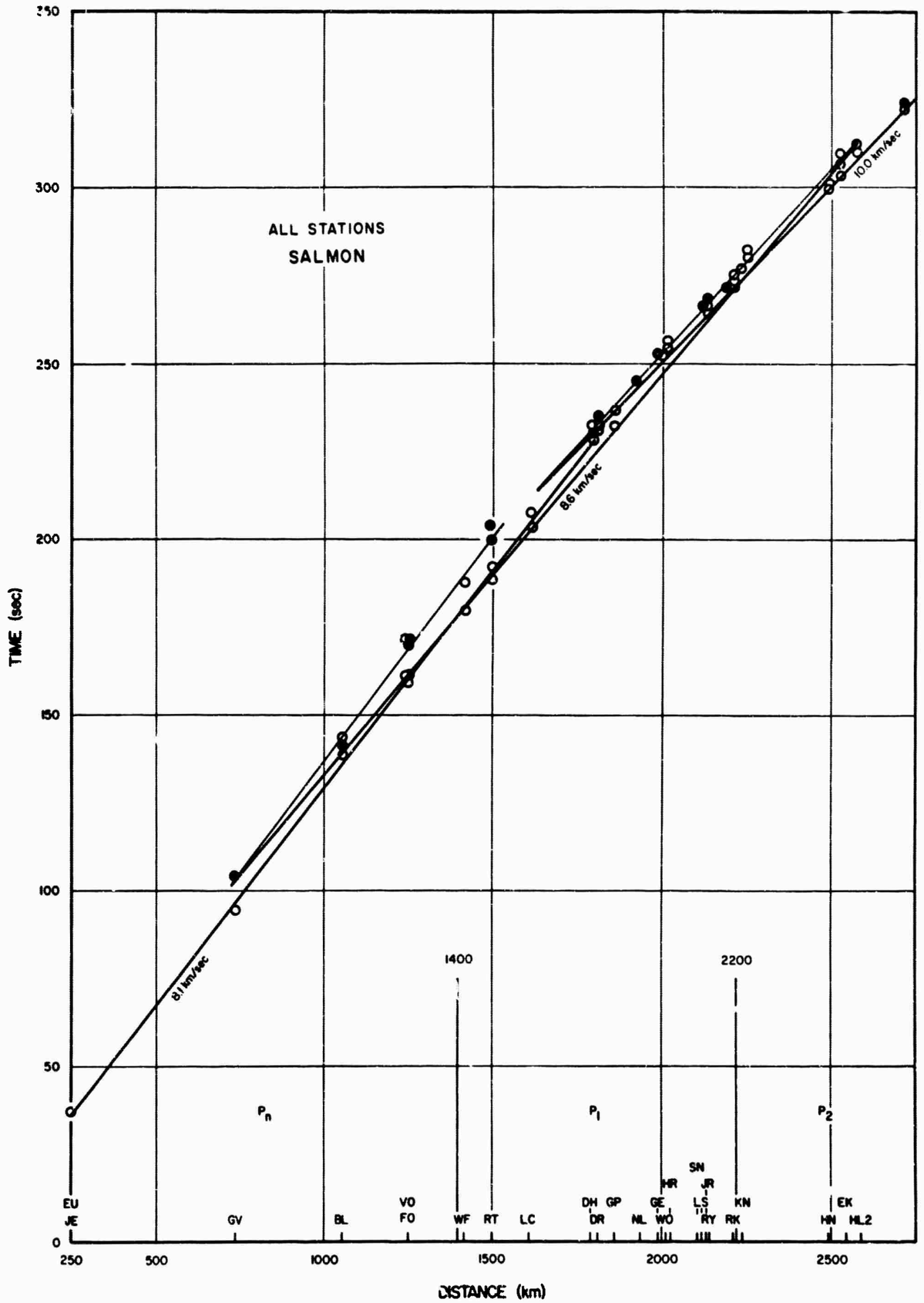

Travel Times versus Distance, All Profiles Combined, SALMON Event

Figure 15

arriving at a particular distance, open circles relatively small or moderate amplitudes. The other symbols refer to J-B travel times.

The travel time curves drawn through the data are based on the travel time data themselves and the previously discussed amplitude-distance spectra. In addition, the curves correspond in their general characteristics to theoretical curves obtained from the velocity structure shown in Figure 16. The initial selection of this structure was based upon a consideration of the long period surface wave dispersion data obtained by a number of investigators and compiled by Anderson and Toksöz.[10] The velocity structure in the mantle is a modified version of the CIT 11 oceanic model proposed by Anderson and Toksöz to explain the Love wave dispersion data. The model has also been found to provide good amplitude and travel time agreement with independent body wave data.

The only extensive modification to their structure is the addition of a crustal section - and of course, conversion to compressional velocities, which involves assumptions of Poisson's ratios. Thus, in view of the essential agreement between continental and oceanic dispersion for periods beyond about 50 seconds, the model agrees with continental long period surface wave dispersion.

While the structure has been checked and perturbed somewhat for consistency with the P phases observed, no particular effort has been made to adjust the fit to the P_n and other body phase data except in an approximate manner. For this reason, the structure shown should be regarded as a preliminary fit, which must be adjusted to account more fully for P_n, the reflected P phases, and the finer details of the direct P phases. In addition, the crustal section used here corresponds to an average crust which, for a finer fit, would have to be replaced by the crustal section appropriate to the particular region or regions involved in the travel time profile.

[10] Anderson, D. L. and Toksöz, M. N., Surface Waves on a Spherical Earth: 1. Upper Mantle Structure from Love Waves: J. Geoph. Res., vol. 68, pp. 3483-3499, 1963.

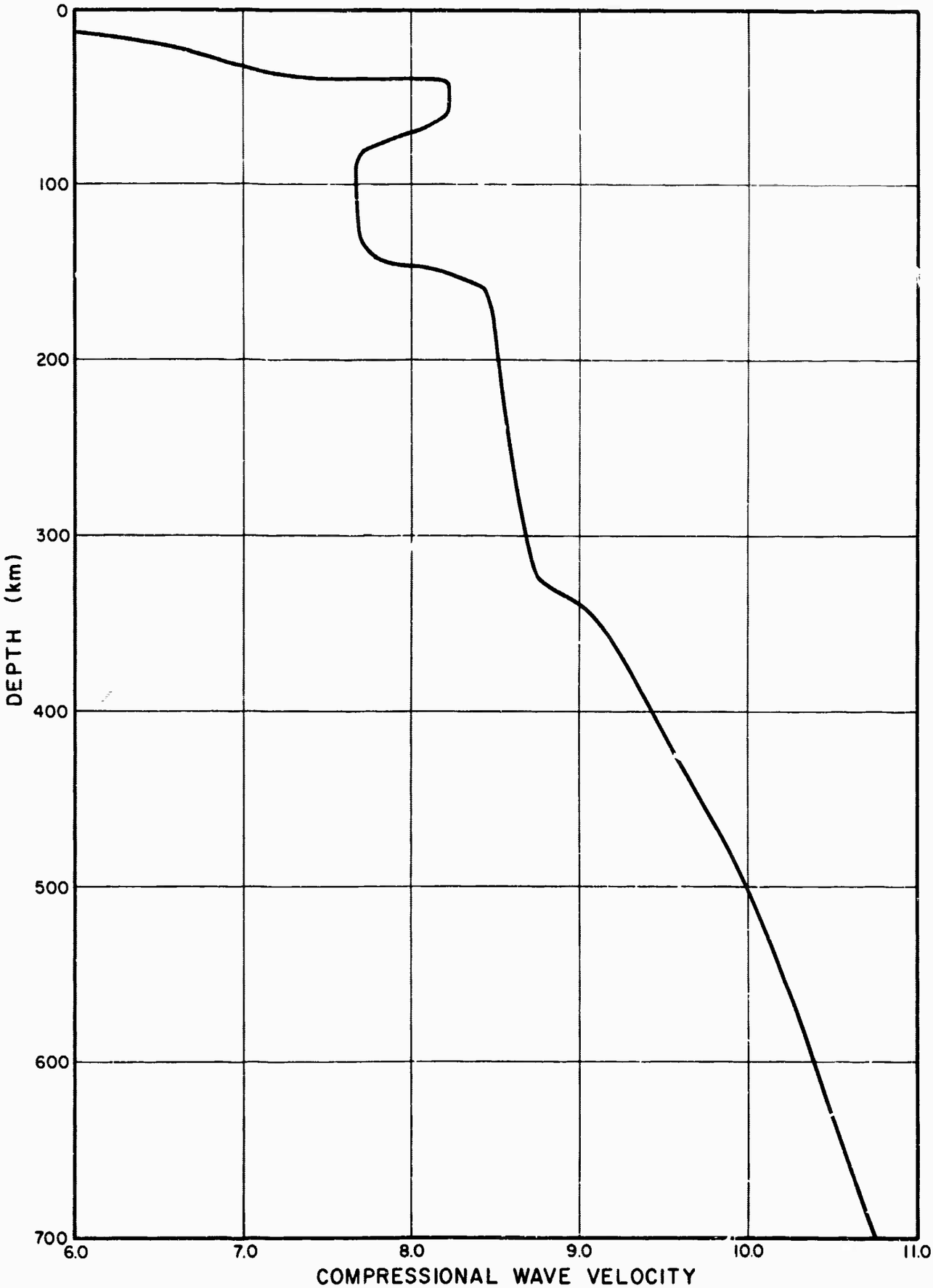

Preliminary Compressional Velocity Structure
to Appropriate Travel Time Observations, SALMON Event

Figure 16

III. WORK IN PROGRESS

Work is continuing on several of the projects discussed in Section II. In addition to these projects, other work in progress at the SDL includes the following items:

A. Inversion of Surface Wave Phase and Group Velocity Dispersion Observations

Preliminary results using the comb-filter program for measuring surface wave group velocity indicate that this is a powerful and sensitive tool for observing crustal and upper mantle structure. In order to utilize fully the potential of the method, an analytical procedure for inverting the observations to find the corresponding best-fitting structure is required.

Following a suggestion of Jeffreys (1961)[11], Archambeau and Anderson [12] derived the inversion coefficients for Love wave phase velocity observations, in terms of the potential and kinetic energy content of the layers comprising the structural mode. Flinn has recently derived inversion coefficient for Rayleigh wave phase velocity, again in terms of layer energies. If the observations are taken, holding frequency instead of wave number constant (as the comb-filter group velocity approach does), the inversion coefficients are layer energy fluxes. As far as phase velocity is concerned, the Rayleigh wave inversion coefficients are exactly as one expects physically: the layer potential energy is split into two parts, a compressional part which affects only the variation of layer bulk modulus, the other part rotational, which affects only the layer rigidity.

Flinn and Archambeau derived expressions for the inversion of Love wave group velocity observations, again in term of layer energies or energy fluxes. The inversion coefficients for Rayleigh wave group velocity are much more complicated, however, and no expression for the corresponding coefficients in terms of layer energies has yet been found.

---

[11] Jeffreys, H., 1961, Small Corrections in the Theory of Surface Waves: Geophy. J., vol. 6, p. 115-117.

[12] Archambeau, C. B., and Anderson, D. L., 1963, Inversion of Surface Wave Dispersion Data: Pub. Bur. Central Seis. Intern., Ser. A., vol. 23, pp. 45-54.

B. Perturbation Theory for the Inversion of Body Wave Travel Time Data

Estimation of the internal elastic structure of the earth from body wave travel times ordinarily uses both arrival time data and the slope of a curve fitted to the observed travel times. There are well known difficulties in fitting such curves, particularly in cases where the observed travel times suggest a multivalued travel time function. A perturbation method has been developed in which an initial velocity distribution, which may be chosen to be in agreement with surface wave dispersion data over the region in question, is pertubed iteratively until the theoretical travel time function is in agreement, in the least-squares sense, with the observed data. The method does not require any estimate of the curve slope or multiplicity, nor does it require a particularly dense and complete data coverage over the entire distance range. Several phases can be used simultaneously.

The initial velocity distribution is taken to be in the form $V(r) = \Sigma a_k f_k(r)$, where the f_k are any set of finite differentiable functions over the appropriate depth range. At each step in the iteration process, variations in the a_k are computed from the travel time residuals δT at fixed distance, from the relation

$$\left(\frac{\delta T}{T}\right)_\Delta = -\sum_k \left(\frac{T_k}{T}\right)_\Delta \left(\frac{\delta a_k}{a_k}\right)$$

where T_k represents a contribution to travel time due to the term $a_k f_k(r)$.

C. Recursive Numerical Filters

The objective of this study is to design a digital computer program that will take conventional filter parameters and automatically design an equivalent recursive digital filter. The parameters used are the poles and numerator polonomial coefficients in the transfer function of the conventional filter. The resultant digital filters are exact in the sense

that their impulse responses are equal to the uniform samples of the impulse responses of their prototype analog filters. More concisely, the objective is to write a computer program to convert Laplace transforms to Z-transforms.

Several intermediate and related results have been obtained. These include the following:

1. A program to compute the frequency response of a conventional filter has been written. This program is used as a check on the digital model in the frequency domain and has been used to check theoretical versus measured frequency responses for seismometer systems.

2. A program to design quadrature filters has been written. These filters are needed to compute analog (and eventually digital) envelope functions. Results using these filters on the analog computer are very good.

3. Recursive models of the elements in a seismic system have been developed.

4. Various recursive Chebychev and Butterworth low-pass filters were designed and compared with their prototypes. Results were good, in general, and an attempt is underway to improve those cases which were not satisfactory.

D. Correlogram Analysis from Linear Arrays

In the past six months correlograms from over a hundred teleseismic earthquake events have been computed for a network of five to ten linear arrays. This analysis is continuing, testing the correlogram method with known signals and various noise samples at selected signal-noise ratios.

E. Dispersion Analysis of Surface Waves from Deep Wall Data

During this reporting period, the digital programs for computing deep well dispersion analyses have been improved. A

theoretical study of this method is nearing completion, and various analyses of deep well data have been made for other investigators.

F. Design of Optimum Arrays

In the project on the optimal design of seismic arrays, the approach has been to consider an array as a discrete approximation to an optimal wave number filter. This wave number filter must be designed from a knowledge of the wave number power spectra of signals and noise. Computer programs have been written to produce these spectra. Studies are in progress to determine the best discrete approximations. Recently, improved methods for obtaining cross power spectra have been incorporated into the wave-number-frequency spectrum program.

G. Partial Coherency Analysis of Seismic Noise

A study is being made of the seismic application of partial coherencies. This study is being carried out jointly with the Measurement Analsyis Corporation under the direction of Dr. Julius Bendat. Organizationally, the participation of MAC is in the role of consultants. The techniques of partial coherencies apply to multichannel filtering problems. By using these methods, multichannel transfer frunctions may be estimated, and tests are possible which determine if the appropriate inputs and outputs have been isolated. The seismic applications will include the analysis of noise in arrays. A preliminary study has been undertaken which demonstrates the numerical computations involved. A report is being prepared on the first phase of the preliminary study. A second report will be concerned with the actual numerical results obtained under controlled conditions. Application is simultaneously being made of these computational tools to seismic data.

H. TFSO Detection Capability Study

Representative noise and seismic signals recorded at TFSO were combined as part of a statistical study of the VELA observatories detection capability. Various combinations of single traces and summation traces are played out on the develocorder and sent to TFO for analysis. A Geotechnical Corporation program is being used to provide a statistical distribution of

the resulting measurements of amplitude and period for different signal levels.

IV. SUPPORT AND SERVICE TASKS

As part of the contract work-statement, the SDL provides support and service functions for AFTAC and other VELA participants. With the approval of AFTAC, the SDL provided one or more of the following services to organizations listed in Appendix A:

- copies of 16 and 35 mm film
- copies of existing composite analog tapes
- composite analog tapes of special events
- use of 1604 computer for checking out new programs or running production programs
- copies of digital programs
- digitized data in standard formats or special formats for use on computers other than the 1604
- running SDL production programs, such as power spectral density, and array processing on specified data
- digital x - y plots of power spectra or digitized data

Visiting scientists have been provided with space to study data and exchange information with SDL personnel.

A. Data Library

The Data Library contains 3400 digitized seismograms, 102 digital computer programs, and 192 composite analog magnetic tapes. This data is available for use by the VELA-UNIFORM program.

The following additions were made during this report period:

1. Digital Seismograms - 1300, including:

   - 10 Lake Superior Explosions
   - Salmon long and short period data
   - noise from several deep wells
   - 16 events recorded on British arrays

- Russian explosions and earthquakes
- array data from over 150 earthquakes

2. Digital Programs - 17, including:

- DEPTHMAG - This program retrieves epicenter information, from punched PDE cards, that meet a certain criteria applied to a number of different values associated with each epicenter. As epicenters are retrieved, the program summarizes on magnitude and depth.

- POINTFLT - This subroutine accepts one data input at a time and passes this data through a set of recursive filter operations which can be stated either as a time operation or as a frequency operation.

- LANDM1 - Given the coefficients of a numerical filter and consecutive segments of an input data series, this routine generates the segments of the corresponding filtered series. The entire series is filtered by means of successive calls to the subroutine.

- TAPMERG2 - To merge two magnetic tapes, made up of epicenter card images on magnetic tape. The resulting merged tape is in chronological sequence and in BCD mode with end-of-files between months and a double-end-of-files at the end of the year.

- COLLATE - This program, using a tape of BCD card images from two different epicenter card lists that are merged into chronological sequence, searches for earthquakes which are reported on both lists. Matching of earthquakes is determined by comparison with (1) a predetermined origin time difference and (2) the

sum of the absolute value of the latitude difference and absolute value of the longitude difference. Latitude, Longitude depth, magnitude, and origin time differences (residuals) are computed only for matched pairs of earthquakes and are available as output.

- TAPEACT - Various EPICENTER cards from several sources are written on tape in a standard format in BCD or packed BINARY mode. SEIS and GEO region numbers may be added into the format. Binary or BCD tapes may be listed at end of an update run or separately. Packed binary tapes (formed by subroutine BCDT2) may be converted back to standard FORTRAN BCD.

- LAGTIME - This program combines a signal and noise on the same data channel at varying signal-to-noise ratios. A tape of the new combination of data is written and a plot tape is formed.

- MAKARAY - Produces a set of output traces corresponding to any set of element positions desired. A noise background is simulated by selecting ten traces from a set of twenty sample traces, and assigning to each an arbitrary velocity, azimuth, and relative amplitude. A signal is selected from a set, its velocity and azimuth are chosen and a signal-to-noise ratio is assigned.

- DISCRETE - Expands either a seismic signal or a specified function in terms of a set of orthonormalized exponential functions. Parameters given by the user define the orthonormal functions. The spectrum of the expansion is available as an option.

- MOD PV-7 FORTRAN - This program computes for all modes of Love and Rayleigh waves on an elastic halfspace of plane-parallel, homogeneous, isotropic layers, the following: phase velocity, group velocity, and surface orbit as functions of period or frequency; amplitude, the product of vertical wave number times layer thickness, and potentials as functions of depth; average kinetic, potential, and total energy densities, and average horizontal energy flux, corresponding to each layer; and a summation of the energy quantities from the free surface. Provision is made for printer plots of phase and group velocity. Provision is also made for partial decoupling where amplitude is large in certain channels at depth, relative to the surface amplitude.

- LOWPAZ - This program performs low pass and high pass filtering of data on a SUBSET format tape, and produces another SUBSET tape and a plot tape of the filtered data.

- FRAMIS - Given the parameters in the LaPlace transform, to evaluate the amplitude spectra and phase of the transformation.

- SORT4 - To sort four arrays in order of increasing or decreasing values of one of them.

- XYPLOT - To plot a function of two variables on the printer.

- RESREC - Computes and plots the amplitude of a recursive phaseless digital filter.

- FLAP - A subordinate control system which allows chaining of programs in any combination to perform a specified analysis.

- PHASDIST - Generates phasing information for an arbitrary array of seismometers, which may be input to the computer program, ARRAY.

Modifications were made to the ARRAY program in order to process array data using the British filtering and smoothing techniques. In addition, modifications were made to the following programs:

1. The analysis of variance program to compute and print X^2.

2. Prediction error filtering program to output results in a form which can then be processed with the analysis of variance program.

3. Program DEPTHMAG to work with different types of input data, and to search and retrieve on the parameter which specifies the source of the magnitude calculation.

3. Analog Composite Tapes - 23, including:

a. Made by Seismic Data Laboratory

- SALMON
- SS VILLAGE
- Russian explosion
- Special composites made for the U. S. Coast & Geodetic Survey, Roland F. Beers, Inc., Texas Instruments, Inc., and Lamont Geophysical Observatory

b. Made by the Geotechnical Corporation

- YUBA
- SATSOP
- KINNEBEC
- GERBIL
- HUTTA
- STONES
- FERRET
- MATACO
- KOHOCTON
- PECAN
- CLEARWATER
- ANCHOVY
- SARDINE
- EAGLE
- GRUNION
- FORE

4. Other Data Available to VELA Participants

The following data is stored on magnetic tape:

- U. S. Coast and Geodetic Survey epi-enters from 1960 to date
- Earthquake Bulletin Data from the LRSM stations (January 1962 to October 1964)
- Earthquake Bulletin Data from the VELA observatories (February 1963 to November 1964)
- Amplitude, period, and arrival times of phases from 50 U. S. shots

B. Digital Computer Operations

The use of digital computer machine data processing techniques for in-house projects and for other VELA participants has been increasing, and recently a second shift digital computer operation was started to handle this increased work-load.

The SDL took over the maintenance of the 1604 digital computer system in January 1965, after a six month period of on-the-job training. Necessary digital spare parts were purchased and a punched card inventory system has been set up for all computer spare parts.

C. Data Compression

This is continuing as a routine operation, and production is maintained at the level needed to meet the requirements of the field operations (LRSM teams and U. S. observatories) and the Seismic Data Laboratory.

D. Equipment Modifications

Six additional Dynamic amplifiers were installed in the playback system to give SDL the capability of making 12 channel playouts with the CEC oscillograph.

The air conditioning system in the computer room was modified so as to be synchronized with the operation of the digital computer.

A cycle adder is being installed on the Sangamo tape transports. This device will permit the SDL to synchronize recording times when processing data simultaneously from two tape recorders.

ORGANIZATIONS RECEIVING SDL DATA SERVICES

OCTOBER 1964 - MARCH 1965

Albuquerque Seismological Center
Bolt, Beranek & Newman, Inc.
Bureau of Standards
California Institue of Tech.
Canadian Dept. of Mines
Engineering Physics
General Atronics Corp.
Geotechnical Corp.
Institue for Meteorology and Geophysics (Germany)
International Seismological Research Centre (Scotland)
Lamont Geological Observatory
Pennsylvania State University
Princeton University
Roland F. Beers Co.
Southwest Center for Advanced Studies
St. Louis University
Texas Instrument, Inc.
Underwater Systems, Inc.
University of California
University of Michigan
University of Sweden
U. S. Coast & Geodetic Survey
Vitro Corporation
Xavier University
Oregon State Univeristy

APPENDIX A

REPORTS ISSUED 1 OCTOBER 1964 THROUGH 31 MARCH 1965

Archambeau, C. B., and Flinn, E. A.; Detection, Analysis, and interpretation of the teleseismic signal from the SALMON event; 2 April 1965.

Booker, A. H.; Analysis of variance as a method for signal detection; 25 February 1965.

Fletcher, N. H., Gerlach, G. S.*; Lobdell, J. L.*, and Wellen, J.B.; The automated bulletin process; 29 March 1965.

Martinek, J., and Thielman, H. P.; Effects of an elastic spherical layer and a liquid core on the propagation of SH waves; 23 February 1965.

Sax, R. L.; General solutions of the wave equation in spherical coordinates for a special class of elastic isotropic inhomogeneous medium; 13 November 1964.

Sax, R. L., and Mims, C. H.; Rectilinear motion detection - REMODE; 22 March 1965.

Staff, SDL; Seismic waves from the SS VILLAGE explosion; 23 November 1964.

Staff, SDL; SALMON; 7 December 1964.

Staff, SDL; Texas-Louisiana earthquake; 9 February 1965.

Staff, SDL; West Virginia earthquake; 1 March 1965.

Van Nostrand, R.; Reverberation effects on signal amplitude; 30 October 1964.

* Geotech

SELECTED REPORTS PREVIOUSLY ISSUED

Booker, A. H.; A statistical discriminator; 22 November 1962.

Booker, A. H.; Estimation of network capability; 20 January 1964.

Booker, A. H.; Parameter dependence of integrated seismic phases; 25 May 1964.

Claerbout, J. F.; Detection of P waves from weak sources at great distances; 13 September 1963.

Dean, W. C.; Inverse filtering of seismic signals; 1 August 1962.

Dean, W. C.; Correlograms of Mississippi from orthogonal filters; 1 March 1963.

Flinn, E. A.; Confidence regions and error determinations for seismic event location; 24 April 1964.

Flinn, E. A. & Engdahl, E. R.*; A proposed basis for geographical and seismic regionalization; 9 March 1964.

Martinek, J., and Thielman, H. P.; Special sphere and circle theorems for the general biharmonic field; 8 July 1963.

Martinek, J. & Thielman, H. P.; Special sphere and circle theorems for the general biharmonic equation - interior and exterior problems; 11 December 1963.

Martinek, J. & Thielman, H. P.; Propagation of waves from a spherical cavity into concentric spheres; 13 March 1964.

Martinek, J., and Thielman, H. P.; Methods for obtaining new solutions to the harmonic and wave equations; 30 April 1964.

Mims, C. H.; A sum-of-squares method of seismic phase identification; 27 November 1962.

* U.S.C. & G.S.

SELECTED REPORTS PREVIOUSLY ISSUED (Continued)

Mims, C. H.; Detectability of first motion; 15 August 1963.

Mitronovas, W.; Identification of nuclear explosions using ratios of smoothed and combined seismic phases; 28 June 1963.

Mitronovas, W.; Identification of nuclear explosions on the shape of initial P-phase for teleseismic events; 28 August 1964.

Pilotte, F. F.*; and Flinn, E. A.; A preliminary evaluation of a method for linear array processing; 31 January 1964.

Sax, R. L.; Attenuation of head waves as a function of frequency and distance; 28 February 1963.

Sax, R. L., and Hartenberger, R. A.; Theoretical estimation of the signal-to-noise ratio as a function of depth; 3 April 1963.

Sax, R. L. and Hartenberger, R. A.: Theoretical prediction of seismic noise in a deep borehole; 24 September 1963.

Sax, R. L., and Hartenberger, R. A.; Seismic noise attenuation in unconsolidated material; 28 August 1964.

Thielman, H. P., and Sax, R. L.; Relation giving the phase velocity in terms of the group velocity; 28 September 1962.

Van Nostrand, R.; Synthetic earthquake seismograms for teleseismic distances; 14 May 1964.

Van Nostrand, R., and Helterbrand, W.*; A comparative study of the SHOAL event; 29 August 1964.

* AFTAC